Bilayer superfluidity of fermionic polar molecules: Many-body effects

M. A. Baranov,[1,2,3] A. Micheli,[1,2] S. Ronen,[1,2] and P. Zoller[1,2]

[1] *Institute for Theoretical Physics, University of Innsbruck, A-6020 Innsbruck, Austria*

[2] *Institute for Quantum Optics and Quantum Information of the Austrian Academy of Sciences, A-6020 Innsbruck, Austria*

[3] *RRC "Kurchatov Institute," Kurchatov Square 1, 123182 Moscow, Russia*

(Received 23 December 2010; published 5 April 2011)

We study the BCS superfluid transition in a single-component fermionic gas of dipolar particles loaded in a tight bilayer trap, with the electric dipole moments polarized perpendicular to the layers. Based on the detailed analysis of the interlayer scattering, we calculate the critical temperature of the interlayer superfluid pairing transition when the layer separation is both smaller (dilute regime) and on the order or larger (dense regime) than the mean interparticle separation in each layer. Our calculations go beyond the standard BCS approach and include the many-body contributions resulting in the mass renormalization, as well as additional contributions to the pairing interaction. We find that the many-body effects have a pronounced effect on the critical temperature and can either decrease (in the very dilute limit) or increase (in the dense and moderately dilute limits) the transition temperature as compared to the BCS approach.

DOI: 10.1103/PhysRevA.83.043602 PACS number(s): 67.85.−d, 03.75.Ss, 74.78.−w

I. INTRODUCTION

Recent experiments have prepared quantum degenerate gases of homonuclear and heteronuclear molecules in electronic and vibrational ground states [1–6]. Heteronuclear molecules, in particular, have large electric dipole moments associated with the rotational excitations, The new feature of polar molecular gases is thus the strong, anisotropic dipole-dipole interactions between the molecules, which can be controlled with external electric fields [7–10]. When dc electric fields are applied to polarize molecules, a major obstacle is given by the increase of inelastic collision rates corresponding to chemical reactions between the molecules, as in the case of KRb in the recent JILA experiments. However, these can be strongly suppressed, and thus the gas stabilized by tightly confining the molecules in a single plane of a quasi-two-dimensional (2D) geometry [11]. This relies on the fact that for induced electric dipole moments perpendicular to the plane of confinement, the dipolar forces will be repulsive in-plane, thus suppressing short-distance inelastic collisions. Such a 2D confinement can be achieved by loading the gas of polar molecules into a one-dimensional (1D) optical lattice. This leads naturally to a setup of a multilayer polar gas where, however, forces between dipoles in different layers can be attractive, and the collapse is prevented by a sufficiently high optical potential barrier. For a bilayer system this attraction can lead to the formation of bound pairs of polar molecules, reminiscent of bilayer excitons, and in a multilayer configuration to the formation of strings of molecules. In particular, in a gas of single-component fermions loaded in a tight bilayer trap, as realized with KRb, this will give rise to an s-wave BCS superfluid transition [12] (for p-wave pairing in a monolayer of polar molecules see Refs. [13] and [14]). It is the purpose of this work to study this bilayer BCS superfluid transition in some detail; in particular we go beyond Ref. [12] with emphasis on the inclusion of many-body effects.

In the bilayer BCS superfluid the single-species polar molecules in the two layers provides the system with a two-component character, where two species are particles on different layers coupled by the long-range dipole interaction, allowing fermions from different layers interact in the s-wave channel that is dominant at low energies. This interlayer interaction results in very peculiar properties in both a two-body system—the existence of interlayer bound states [15–18] and various regimes of the interlayer scattering [18]—and in a many-body system—interlayer BCS pairing [12] and BCS-BEC (Bose-Einstein condensation) crossover [12,19]. Based on a detailed analysis of various regimes of interlayer and intralayer scattering, we extend the analysis of the interlayer superfluid pairing beyond the standard BCS approach [12] by including many-body contributions resulting in the mass renormalization, as well as in additional contributions to the pairing interaction. We perform the calculation of the critical temperature in the regime of a weak interlayer coupling for the cases when the layer separation is both smaller (dilute regime) and on the order or larger (dense regime) than the mean interparticle separation in each layer. As found, the many-body effects have a pronounced effect on the critical temperature and could either decrease (in the very dilute limit) or increases (in the dense and moderately dilute limits) the transition temperature as compared to the BCS approach.

The paper is organized as follows: Sec. II gives an overview of the problem and identifies the relevant parameters and parameter regimes. In Sec. III we introduce the model describing bilayer pairing. Section IV discusses two-particle bound states and scattering properties for the interlayer problem. Section V provides a theoretical treatment of many-body effects in interlayer BCS pairing. Results for the critical temperature in the dilute and dense limit are summarized in Secs. VI and VII, respectively.

II. OVERVIEW OF THE PROBLEM AND SUMMARY OF THE RESULTS

The considered single-component fermionic bilayer dipolar system provides an example of a relatively simple many-body system in which an entire range of nontrivial many-body phenomena are solely tied to the dipole-dipole interparticle interaction with its unique properties: long-range and anisotropy. The long-range character provides an interparticle interaction in single-component Fermi gases inside each layer that otherwise would remain essentially noninteracting. For the considered setup, this intralayer interaction is always repulsive and gives rise to the crystalline phase for a large density of particles. More important, the long-range dipole-dipole interaction couples particles from different layers in a very specific form resulting from the anisotropy of the interaction: Two particles from different layers attract each other at short and repel each other at large distances, respectively, as a result of different mutual orientations of their relative coordinate and of their dipole moments. The potential well at short distances is strong enough to support at least one bound state for any strength of interlayer coupling. For a weak coupling between layers, the bound state is extremely shallow and has an exponentially large size. However, in the intermediate and strong coupling cases the size of the deepest bound state becomes comparable with the interlayer separation. In the fermionic many-body system this behavior of the interlayer interaction leads to a BCS state with interlayer Cooper pairs in the weak (interlayer) coupling regime when the size of the bound state is larger than the interparticle separation (in other words, the Fermi energy is larger than the binding energy). With increasing interlayer coupling, this BCS state smoothly transforms into a BEC state of tightly bound interlayer molecules when the interparticle separation is larger than the size of the bound state. Of course, the BEC regime and BEC-BCS crossover are possible only when the mean interparticle separation in each layer is larger than the distance between the layers.

In this paper we focus on the regime of weak intra- and interlayer interactions, which allows the usage of controllable calculations on the basis of the perturbation theory, and consider in detail the formation of the interlayer BCS state. Before entering the technical derivation, it seems worthwhile to briefly identify the relevant parameters and parameter regimes for the bilayer many-body system of single-species fermionic dipoles. In addition, we will point out where the relevant results and discussions for these parameter regimes can be found in later parts of the paper.

It follows from the previous discussion that the considered system is characterized by three characteristic lengths: the dipolar length $a_d = md^2/\hbar^2$, where m is the mass of dipolar particles with the (induced) dipole moment d, the interlayer separation l, and the mean interparticle separation inside each layer $\sim k_F^{-1}$ with $k_F = \sqrt{4\pi n}$ being the Fermi wavevector for a 2D single-component fermionic gas with the density n. Therefore, the physics of the system is completely determined by two dimensionless parameters that are independent ratios of the above lengths.

The first parameter g is the ratio of the dipolar length and the interlayer separation, $g = a_d/l$, and is a measure of the interlayer interaction strength relevant for pairing. In experiments with polar molecules, the values of the dipolar length a_d are on the order of 10^2–10^4 nm: For a ^{40}K^{87}Rb with currently available $d \approx 0.3$ D one has $a_d \approx 170$ nm (with $a_d \approx 600$ nm for the maximum value $d \approx 0.566$ D), and for ^{6}Li^{133}Cs with the tunable dipole moment from $d = 0.35$ to 1.3 D in an external electric field $\sim$1 kV/cm the value of a_d varies from $a_d \approx 260$ to ≈ 3500 nm. For the interlayer separation $l = 500$ nm these values of a_d correspond to $g \lesssim 10$.

The second parameter $k_F l$ measures the interlayer separation in units of the mean interparticle distance in each layer. This parameter can also be both smaller (dilute regime) and on the order or larger (dense regime) than unity for densities $n = 10^6$–10^9 cm^{-2} (for example, for $l = 500$ nm one has $k_F l = 1$ for $n \approx 3 \times 10^7$ cm^{-2}).

The two parameters g and $k_F l$ determine the regime of interlayer scattering at typical energies of particles ($\sim$ Fermi energy $\varepsilon_F = \hbar^2 k_F^2/2m$), and their product, $g k_F l = a_d k_F$, being the ratio of the dipolar length and the mean interparticle separation inside each layer, controls the perturbative expansion in the system and, therefore, many-body effects. The existence of different regimes of the interlayer scattering originates from two characteristic features of the interlayer dipole-dipole interaction, as discussed in the context of Eq. (4) below: the presence of the typical range $\sim l$ beyond which the interaction is attractive and of the long-range dipole-dipole repulsive tail. As a result, the Fourier component of the interaction [see Eq. (8) below] decays exponentially for large momentum $k \gg l^{-1}$, while it is proportional to k for $k \ll l^{-1}$ and, hence, vanishes for $k = 0$. This leads to three different regimes of scattering and, therefore, of the BCS pairing, depending on the relation between g and $k_F l$: regime A when $g < k_F l \lesssim 1$, regime B when $\exp(-1/g^2) \ll k_F l < g < 1$, and regime C when $\exp(-1/g^2) \lesssim k_F l \ll g < 1$. The exponential factor in the last two formulas is related to the size of an extremely shallow (in the limit of small g) interlayer bound state [see Eq. (11) below].

A. Regime A: $g < k_F l \lesssim 1$

In this regime $g < k_F l \lesssim 1$, and the scattering is dominated by the first Born approximation [see Eqs. (18) and (25) for the s-wave scattering amplitude for $k_F l \ll 1$ and $k_F l \lesssim 1$, respectively]. The critical temperature in this case will be given below in Eqs. (57) and (78) for the dilute, $k_F l \ll 1$, and the dense, $k_F l \lesssim 1$ cases, respectively. The ratio of the critical temperature to the Fermi energy (chemical potential), T_c/ε_F, can reach in this regime values on the order of 0.1 (see Fig. 7), making an experimental realization of the interlayer BCS pairing very promising. Note that the maximum of the ration T_c/ε_F corresponds to $k_F l \approx 0.5$.

B. Regime B: $\exp(-1/g^2) \ll k_F l < g < 1$

In regime B, $\exp(-1/g^2) \ll k_F l < g < 1$, the interlayer scattering is dominated by the second-order Born contribution [see Eq. (19)], and the critical temperature will be given below in Eq. (62).

C. Regime C: $\exp(-1/g^2) \lesssim k_F l \ll g < 1$

Finally, in regime C, $\exp(-1/g^2) \lesssim k_F l \ll g < 1$, we recover the universal behavior for a 2D low-energy scattering [see Eq. (20)], with the typical inverse-logarithmic dependence of the s-wave scattering amplitude on the energy. The critical temperature is provided by Eq. (63) and coincides with the critical temperature in a two-component gas with a short-range interaction with the same Fermi energy and the bound-state energy. Note that the values of the critical temperature in regimes B and C are much smaller ($T_c/\varepsilon_F \lesssim 10^{-3}$) than in regime A. This makes an experimental realization of the interlayer pairing in these regimes very challenging.

III. THE MODEL

We consider a system of single-component polarized fermionic dipolar particles (harmonically) confined in two infinite quasi-2D layers separated by a distance l, which is much larger than the confinement length l_0 in each layer, $l \gg l_0$. We assume that each layer has the same density n of dipolar particles with mass m and dipolar moment d polarized along the z axis, which is perpendicular to the layers (see Fig. 1). The Hamiltonian of the system reads

$$H = \sum_{\alpha=\pm}\int d\mathbf{r}\hat{\psi}_\alpha^\dagger(\mathbf{r})\left\{-\frac{\hbar^2}{2m}\Delta + \frac{1}{2}m\omega_z^2 z_\alpha^2 - \mu'\right\}\hat{\psi}_\alpha(\mathbf{r}) + \frac{1}{2}\sum_{\alpha,\beta}\int d\mathbf{r}d\mathbf{r}'\hat{\psi}_\alpha^\dagger(\mathbf{r})\hat{\psi}_\beta^\dagger(\mathbf{r}')V(\mathbf{r}-\mathbf{r}')\hat{\psi}_\beta(\mathbf{r}')\hat{\psi}_\alpha(\mathbf{r}), \tag{1}$$

where $\alpha = \pm$ is the layer index, $z_\pm \equiv z \pm l/2$, $\hat{\psi}_\alpha(\mathbf{r})$ with $\mathbf{r} = (\boldsymbol{\rho},z)$ is the field operator for fermionic dipolar particles ($\boldsymbol{\rho} = x\mathbf{e}_x + y\mathbf{e}_y$) on the corresponding layer α, $\Delta = \Delta_{\boldsymbol{\rho}} + \partial^2/\partial_z^2$ is the Laplace operator, ω_z is the confining frequency in each layer such that $l_0 = \sqrt{\hbar/m\omega_z}$, and μ' is the chemical potential. The last term with

$$V(\mathbf{r}) = \frac{d^2}{r^3}\left(1 - 3\frac{z^2}{r^2}\right)$$

describes the intra- ($\alpha = \beta$) and interlayer ($\alpha \neq \beta$) dipole-dipole interparticle interactions. Assuming a strong confinement, $\hbar\omega_z \gg \mu', T$, where T is the temperature, we can write

$$\hat{\psi}_\alpha(\mathbf{r}) = \hat{\psi}_\alpha(\boldsymbol{\rho})\phi_0(z_\alpha) \equiv \hat{\psi}_\alpha(\boldsymbol{\rho})\frac{e^{-z_\alpha^2/2l_0^2}}{(\sqrt{\pi}l_0)^{1/2}}$$

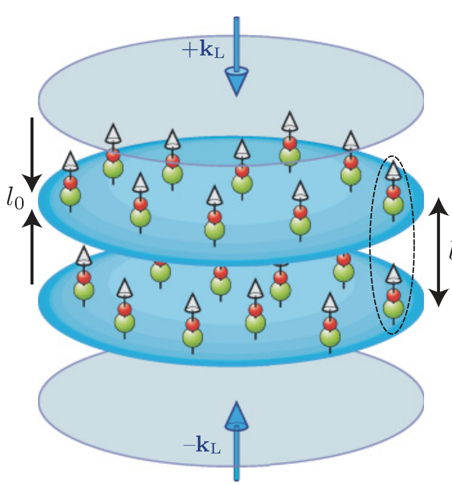

FIG. 1. (Color online) The setup of the dipolar bilayer system: Two layers with the thickness l_0 of a 1D optical lattice formed by two counterpropagating laser waves with wavevectors $\mathbf{k}_L$ and $-\mathbf{k}_L$ are filled with dipoles oriented perpendicular to the layers. The interlayer distance l is π or k_L. An interlayer Cooper pair or molecule is schematically indicated by the dashed oval.

and, therefore, reduce the Hamiltonian (1) to

$$H_{2D} = \sum_{\alpha=\pm}\int d\boldsymbol{\rho}\hat{\psi}_\alpha^\dagger(\boldsymbol{\rho})\left\{-\frac{\hbar^2}{2m}\Delta_{\boldsymbol{\rho}} - \mu\right\}\hat{\psi}_\alpha(\boldsymbol{\rho}) + \frac{1}{2}\sum_{\alpha,\beta}\int d\boldsymbol{\rho}d\boldsymbol{\rho}'\hat{\psi}_\alpha^\dagger(\boldsymbol{\rho})\hat{\psi}_\beta^\dagger(\boldsymbol{\rho}') \times V_{\alpha\beta}(\boldsymbol{\rho}-\boldsymbol{\rho}')\hat{\psi}_\beta(\boldsymbol{\rho}')\hat{\psi}_\alpha(\boldsymbol{\rho}), \tag{2}$$

for a two-component fermionic field $\hat{\psi}_\alpha(\boldsymbol{\rho})$, $\alpha = \pm$, with shifted chemical potential $\mu = \mu' - \hbar\omega_z/2$.

The intracomponent (intralayer) interaction is

$$\begin{aligned}V_{\alpha\alpha}(\boldsymbol{\rho}) &= \int dz\,dz'\,V(\mathbf{r}-\mathbf{r}')\,\phi_0^2(z_\alpha)\,\phi_0^2(z'_\alpha) \\ &= \frac{d^2}{\sqrt{2\pi}l_0^3}\int_0^\infty d\xi\sqrt{\frac{\xi}{(\xi+1)^3}}\exp\left(-\xi\frac{\rho^2}{l_0^2}\right) \\ &= \frac{d^2}{\sqrt{8\pi}l_0^3}\exp\left(-\frac{\rho^2}{4l_0^2}\right) \\ &\quad\times\left[\left(2+\frac{\rho^2}{l_0^2}\right)K_0\left(\frac{\rho^2}{4l_0^2}\right) - \frac{\rho^2}{l_0^2}K_1\left(\frac{\rho^2}{4l_0^2}\right)\right],\end{aligned} \tag{3}$$

where $K_n(z)$ is the modified Bessel functions, and the intercomponent (interlayer) one

$$V_{+-}(\boldsymbol{\rho}) = V_{-+}(\boldsymbol{\rho}) \equiv V_{2D}(\boldsymbol{\rho}) \approx d^2\frac{\rho^2 - 2l^2}{(\rho^2+l^2)^{5/2}}. \tag{4}$$

The intralayer interaction V_{++} is purely repulsive:

$$V_{++}(\boldsymbol{\rho}) \approx \begin{cases} d^2/\rho^3 & \text{for} \quad \rho \gg l_0 \\ (\sqrt{2/\pi})(d^2/l_0^3)\ln(l_0/\rho) & \text{for} \quad \rho \ll l_0 \end{cases}.$$

As a result, if the density n is not too large (such that particles in each layer are in a gas phase [20,21]), it leads only to Fermi liquid renormalization of the parameters of the Hamiltonian (2) (effective mass, for example). The corresponding Fourier transform reads

$$\tilde{V}_{++}(\mathbf{k}) = \sqrt{2\pi}\frac{4}{3}\frac{d^2}{l_0} + \tilde{V}'_{++}(\mathbf{k}), \tag{5}$$

where

$$\tilde{V}'_{++}(\mathbf{k}) = -2\pi d^2 k\exp\left(k^2l_0^2/2\right)[1 - \mathrm{erf}(kl_0/\sqrt{2})]$$

with $\mathrm{erf}(z) = (2/\sqrt{\pi})\int_0^x ds e^{-s^2}$ being the error function. In the considered limit $kl_0 \ll 1$, one simply has

$$\tilde{V}'_{++}(\mathbf{k}) \approx -2\pi d^2 k = -\frac{2\pi\hbar^2}{m}gkl. \tag{6}$$

The effect of the interlayer interaction $V_{2D}(\boldsymbol{\rho})$ (see Fig. 2) is more interesting.

A peculiar property of $V_{2D}(\boldsymbol{\rho})$ is

$$\int d\boldsymbol{\rho}V_{2D}(\boldsymbol{\rho}) = 0. \tag{7}$$

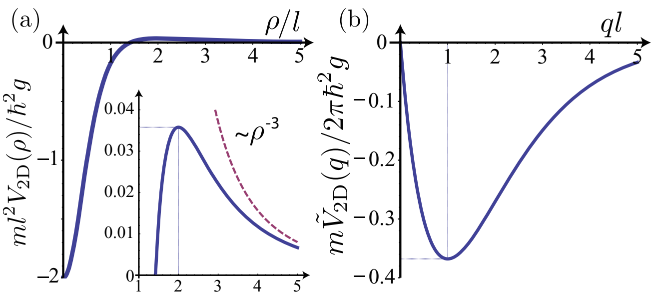

FIG. 2. (Color online) The interlayer potential $V_{+-}(\rho) = V_{2D}(\rho)$ and its Fourier transform $\tilde{V}_{2D}(q)$.

This means that its Fourier transform

$$\tilde{V}_{2D}(\mathbf{q}) = \int d\boldsymbol{\rho} V_{2D}(\boldsymbol{\rho}) e^{-i\mathbf{q}\boldsymbol{\rho}} = -\frac{2\pi\hbar^2}{m} gql e^{-ql} \tag{8}$$

vanishes for small q,

$$\tilde{V}_{2D}(\mathbf{q} \to \mathbf{0}) \approx -\frac{2\pi\hbar^2}{m} gql \to 0.$$

Hence, for sufficiently small energies, the interparticle scattering will be dominated by higher-order contributions in the Born expansion. Note also that the linear dependence of $\tilde{V}_{2D}(\mathbf{q})$ on q for $ql \ll 1$ is the consequence of the long-range power decay of $V_{2D}(\boldsymbol{\rho})$ for large ρ (the so-called anomalous contribution to scattering; see Ref. [22]). Another consequence of Eq. (7) is that the interlayer bound state, which always exists in the potential $V_{2D}(\boldsymbol{\rho})$ [15–18], has extremely low binding energy for $g \ll 1$.

From the point of view of many-body physics, however, the crucial observation is that $\tilde{V}_{2D}(\mathbf{q})$ is negative for all q, signaling the possibility of the interlayer pairing in the form of BCS pairs when the size of the interlayer bound state R_b is much larger than the interparticle separation, $R_b \gg n^{-1/2}$, or in the form of interlayer dimers for $R_b < n^{-1/2}$ with some crossover in between (analogous to the BEC-BCS crossover in 2D and 3D for two-component Fermi gases with short-range interactions).

The Hamiltonian (2) is characterized by two parameters: $g = md^2/\hbar^2 l$, which is the ratio of the dipolar length $a_d = md^2/\hbar^2$ and the interlayer spacing l, and $k_F l$, where $k_F = (2\pi n)^{1/2}$ is the Fermi wavevector ($p_F = \hbar k_F$ is the Fermi momentum), which is the ratio of the interlayer spacing l and the average interparticle separation in each layer. Note that the quantity $gk_F l = a_d k_F$ measures the strength of the intralayer dipole-dipole interaction energy $d^2 n^{3/2} \sim d^2 k_F^3$ to the mean kinetic energy of particles $\sim\varepsilon_F = \hbar^2 k_F^2/2m$. In this paper we consider weakly interacting gas of dipolar particles with $gk_F l < 1$ in the dilute $k_F l < 1$ and dense $k_F l \gtrsim 1$ regimes.

IV. THE INTERLAYER TWO-BODY PROBLEM: BOUND STATES AND SCATTERING PROPERTIES

Let us first discuss the bound state and the scattering of two particles interacting with the potential $V_{2D}(\rho)$ interlayer two-body problem (this problem was also addressed in Ref. [18]; see, however, discussion below). For this purpose we have to solve the 2D Schrödinger equation for the relative motion wavefunction $\psi(\boldsymbol{\rho})$

$$\left\{-\frac{\hbar^2}{2m_r}\Delta_{\boldsymbol{\rho}} + V_{2D}(\boldsymbol{\rho})\right\}\psi(\boldsymbol{\rho}) = E\psi(\boldsymbol{\rho}), \tag{9}$$

where $m_r = m/2$ is the reduced mass and the function $\psi(\boldsymbol{\rho})$ is regular for $\boldsymbol{\rho} \to 0$. For the bound-state solution with $E = -E_b < 0$, the wavefunction $\psi(\boldsymbol{\rho})$ should decay exponentially for large ρ, while for the scattering wavefunction $\psi_{\mathbf{k}}^{(+)} \cdot (\boldsymbol{\rho})$ with $E = \hbar^2 k^2/m > 0$, the boundary condition for large ρ reads

$$\psi_{\mathbf{k}}^{(+)}(\boldsymbol{\rho}) \approx \exp(i\mathbf{k}\cdot\boldsymbol{\rho}) - \frac{f_k(\varphi)}{\sqrt{-8\pi i k\rho}} \exp(ik\rho),$$

where $f_k(\varphi)$ is the scattering amplitude and φ is the azimuthal angle, $\mathbf{k}\cdot\boldsymbol{\rho} = k\rho\cos(\varphi)$. (Our definition of the scattering amplitude corresponds to that of Ref. [23], which is differs by a factor of $-\sqrt{8\pi k}$ from the definition of Ref. [22].)

A. Bound state

Writing the wavefunction for the relative motion of two particles in the form

$$\psi(\boldsymbol{\rho}) = \chi_{m_z}(\rho)\exp(im_z\varphi),$$

where m_z is the magnetic quantum number, we obtain the following equation for the radial wavefunction $\chi_{m_z}(\rho)$ of the bound state with the binding energy E_b:

$$\left[\frac{d^2}{d\rho^2} + \frac{1}{\rho}\frac{d}{d\rho} - \frac{m_z^2}{\rho^2} - \frac{E_b + V_{2D}(\rho)}{\hbar^2/m}\right]\chi_{m_z}(\rho) = 0, \tag{10}$$

and the function $\chi_{m_z}(\rho)$ should be regular for $\rho \to 0$ and decays exponentially for large ρ.

It is sufficient for our purposes to consider the azimuthally symmetric case $m_z = 0$, for which we consider two limiting cases $g \gg 1$ and $g \ll 1$. In the first case, the potential $V_{2D}(\rho)$ supports several ($\sim g^{1/2}$) bound states, and the lowest bound state has the binding energy $E_b = (\hbar^2/ml^2)2g(1 - \sqrt{6/g})$ and $R_b \sim l(6g)^{-1/4}$. In the opposite limit $g \ll 1$, there is only one shallow bound state (the existence of this bound state was proven in Ref. [15]) with the binding energy; see details of the derivation in Appendix A:

$$E_b \approx \frac{4\hbar^2}{ml^2}\exp\left[-\frac{8}{g^2} + \frac{128}{15g} - \frac{2521}{450} - 2\gamma + O(g)\right], \tag{11}$$

where $\gamma \approx 0.5772$ is the Euler constant, and with the size

$$R_b \approx \sqrt{\hbar^2/mE_b} \sim l\exp(4/g^2) \gg l.$$

Note that the expression (11) for the binding energy coincides with the corresponding one given in Ref. [18] only to the leading order ($\sim 1/g^2$). This is because the next-order terms in the exponent ($\sim g^{-1}$ and $\sim g^0$) are determined by the terms of the third and fourth orders in g in the scattering amplitude (or in the wavefunction), respectively (see Appendix A). In Ref. [18], however, only terms up to second order were taken into account, and, therefore, only the leading term is correct; see Figs. 8 and 9.

B. Scattering

For the analysis of scattering it is convenient to introduce the vertex function $\Gamma(E,\mathbf{k},\mathbf{k}')$, where the arguments E, $\mathbf{k}$, and $\mathbf{k}'$ are independent of each other. This function satisfies the following integral equation [24]:

$$\Gamma(E,\mathbf{k},\mathbf{k}') = V_{2D}(\mathbf{k}-\mathbf{k}') + \int \frac{d\mathbf{q}}{(2\pi)^2} V_{2D}(\mathbf{k}-\mathbf{q}) \times \frac{1}{E-\hbar^2 q^2/m + i0}\Gamma(E,\mathbf{q},\mathbf{k}'). \qquad (12)$$

The off-shell scattering amplitude

$$f_{\mathbf{k}}(\mathbf{k}') = \frac{m}{\hbar^2}\int d\boldsymbol{\rho}\,\exp(-i\mathbf{k}'\boldsymbol{\rho})V_{2D}(\boldsymbol{\rho})\psi^{(+)}_{\mathbf{k}}(\boldsymbol{\rho})$$

with $k \neq k'$ can be obtained from $(m/\hbar^2)\Gamma(E,\mathbf{k},\mathbf{k}')$ by putting $E = \hbar^2 k^2/m$, and the scattering amplitude $f_k(\varphi)$, where φ is the angle between $\mathbf{k}$ and $\mathbf{k}'$, corresponds to $(m/\hbar^2)\Gamma(E,\mathbf{k},\mathbf{k}')$ with $E = \hbar^2 k^2/m = \hbar^2 k'^2/m$.

The iteration of Eq. (12) up to the fourth-order term in $\tilde{V}_{2D}(\mathbf{q})$ reads

$$\begin{aligned}\Gamma(E,\mathbf{k},\mathbf{k}') &= \tilde{V}_{2D}(\mathbf{k}-\mathbf{k}') + \int \frac{d\mathbf{q}}{(2\pi)^2}\frac{\tilde{V}_{2D}(\mathbf{k}-\mathbf{q})\tilde{V}_{2D}(\mathbf{q}-\mathbf{k}')}{E-\hbar^2q^2/m+i0} + \int \frac{d\mathbf{q}_1 d\mathbf{q}_2}{(2\pi)^4}\frac{\tilde{V}_{2D}(\mathbf{k}-\mathbf{q}_1)\tilde{V}_{2D}(\mathbf{q}_1-\mathbf{q}_2)\tilde{V}_{2D}(\mathbf{q}_2-\mathbf{k}')}{\left(E-\hbar^2q_1^2/m+i0\right)\left(E-\hbar^2q_2^2/m+i0\right)}\\ &\quad + \int \frac{d\mathbf{q}_1 d\mathbf{q}_2 d\mathbf{q}_3}{(2\pi)^6}\frac{\tilde{V}_{2D}(\mathbf{k}-\mathbf{q}_1)\tilde{V}_{2D}(\mathbf{q}_1-\mathbf{q}_2)\tilde{V}_{2D}(\mathbf{q}_2-\mathbf{q}_3)\tilde{V}_{2D}(\mathbf{q}_3-\mathbf{k}')}{\left(E-\hbar^2q_1^2/m+i0\right)\left(E-\hbar^2q_2^2/m+i0\right)\left(E-\hbar^2q_3^2/m+i0\right)} + \cdots\\ &\equiv \Gamma^{(1)}(E,\mathbf{k},\mathbf{k}') + \Gamma^{(2)}(E,\mathbf{k},\mathbf{k}') + \Gamma^{(3)}(E,\mathbf{k},\mathbf{k}') + \Gamma^{(4)}(E,\mathbf{k},\mathbf{k}') + \cdots. \end{aligned} \qquad (13)$$

We now estimate the leading contributions of these terms in the small energy limit $k \sim k' \sim \sqrt{mE/\hbar^2} \ll 1/l$:

$$\Gamma^{(1)}(E,\mathbf{k},\mathbf{k}') = \tilde{V}_{2D}(\mathbf{k}-\mathbf{k}') \approx -\frac{2\pi\hbar^2}{m} g|\mathbf{k}-\mathbf{k}'|l, \qquad (14)$$

$$\Gamma^{(2)}(E,\mathbf{k},\mathbf{k}') \approx -\frac{2\pi\hbar^2}{m}\frac{g^2}{4}, \qquad (15)$$

$$\Gamma^{(3)}(E,\mathbf{k},\mathbf{k}') \approx -\frac{2\pi\hbar^2}{m}\frac{4g^3}{15}, \qquad (16)$$

$$\Gamma^{(4)}(E,\mathbf{k},\mathbf{k}') \approx -\frac{2\pi\hbar^2}{m}\frac{g^4}{32}[\ln(\hbar^2/mEl^2) + i\pi]. \qquad (17)$$

The estimate for $\Gamma^{(1)}$ is trivial, the leading contributions to $\Gamma^{(2)}$ and $\Gamma^{(3)}$ come from large q ($q \gg k$) and large q_1, q_2 ($q_i \gg k$) regions, respectively, and the leading contributions to $\Gamma^{(4)}$ originate from large q_1 ($q_1 \gg k$) and q_3 ($q_3 \gg k$) but small q_2 ($q_2 \sim \sqrt{mE/\hbar^2}$). Note that the next-order terms (except those for $\Gamma^{(1)}$) have relative magnitude on the order of $(kl)^2\ln(kl)$.

As already noted in Sec II. the above estimates show that there are three different regimes of scattering for $g < 1$ and $kl < 1$ (dilute weakly interacting regime for a many-body fermionic system with $k \sim k_F$ and $E \sim \varepsilon_F$): (a) $g < kl < 1$, (b) $\exp(-1/g^2) \ll kl < g < 1$, and (c) $\exp(-1/g^2) \lesssim kl \ll g < 1$.

Regime A. The leading contribution to scattering is given by the first Born term,

$$\Gamma_a(E,\mathbf{k},\mathbf{k}') \approx \Gamma^{(1)}(E,\mathbf{k},\mathbf{k}') \approx -\frac{2\pi\hbar^2}{m} g|\mathbf{k}-\mathbf{k}'|l, \qquad (18)$$

valid for $g < kl < 1$.

Regime B. The scattering in this case is dominated by the second-order Born contribution,

$$\Gamma_b(E,\mathbf{k},\mathbf{k}') \approx \Gamma^{(2)}(E,\mathbf{k},\mathbf{k}') \approx -\frac{2\pi\hbar^2}{m}\frac{g^2}{4}, \qquad (19)$$

valid for $\exp(-1/g^2) \ll kl < g < 1$. In this case the scattering amplitude is momentum and energy independent and, hence, is equivalent to a pseudopotential $V_0(\boldsymbol{\rho}) = -(2\pi\hbar^2/m)(g^2/4)\delta(\boldsymbol{\rho})$.

Regime C. In this case the second- and the fourth-order contributions become of the same order, and one has to sum leading contributions from the entire Born series. The result of this summation is

$$\Gamma_c(E,\mathbf{k},\mathbf{k}') \approx \frac{2\pi\hbar^2}{m}\frac{2}{\ln(E_b/E) + i\pi}, \qquad (20)$$

valid for $\exp(-1/g^2) \lesssim kl \ll g < 1$, where E_b is the energy of the bound state from Eq. (11). This expression recovers the standard energy dependence of the 2D low-energy scattering. The scattering amplitude $\Gamma_c(E,\mathbf{k},\mathbf{k}')$ has a pole at $E = -E_b$, as it should, and the real part of $\Gamma_c(E,\mathbf{k},\mathbf{k}')$, being zero at $E = E_b$, changes from negative to positive values for $E > E_b$ and $E < E_b$, respectively. Note that within the lowest-order terms, one can write a unique expression for the scattering amplitude for the three regimes in the form (for more details see Appendix A)

$$\Gamma(E,\mathbf{k},\mathbf{k}') \approx -\frac{2\pi\hbar^2}{m}\left[g\left|\mathbf{k}-\mathbf{k}'\right| l - \frac{2}{\ln(E_b/E) + i\pi}\right].$$

For later discussion we note that the scattering amplitude has both real and imaginary parts. The relation between them can be established on the basis of Eq. (12) by considering the imaginary part of both sides of the equation

$$\mathrm{Im}\Gamma(E,\mathbf{k},\mathbf{k}') = -\frac{m}{4\hbar^2}\int \frac{d\varphi_{\mathbf{q}}}{2\pi}\Gamma^*(E,\mathbf{k},\mathbf{q}_E)\Gamma(E,\mathbf{q}_E,\mathbf{k}'), \qquad (21)$$

where $|\mathbf{q}_E| = \hbar^{-1}\sqrt{mE}$, the integration is performed over the direction of this vector, and the complex conjugate amplitude $\Gamma^*(E,\mathbf{k},\mathbf{k}')$ obeys Eq. (12) with $-i0$ in the denominator of the integral term. This relation results in the unitarity condition for the scattering matrix (optical theorem), and its validity in the second order of the perturbation theory is demonstrated in Appendix D. The analog of Eq. (21) for partial wave scattering amplitudes $\Gamma_m(E,k,k')$ with azimuthal (magnetic) quantum number m follows from Eq. (21) after integrating over the directions of $\mathbf{k}$ and $\mathbf{k}'$ with the proper angular harmonic. As an example, for the s-wave scattering channel with

$$\Gamma_s(E,k,k') = \langle \Gamma(E,\mathbf{k},\mathbf{k}')\rangle_{\varphi,\varphi'} \tag{22}$$

we obtain

$$\mathrm{Im}\Gamma_s(E,k,k') = -\frac{m}{4\hbar^2}\Gamma_s^*(E,k,q_E)\Gamma_s(E,q_E,k').$$

On the mass shell, $k = k' = q_E = \hbar^{-1}\sqrt{mE}$, the above relation reads

$$\mathrm{Im}\Gamma_s(k) = -\frac{m}{4\hbar^2}\,|\Gamma_s(k)|^2\,. \tag{23}$$

This implies that up to the second order one has

$$\mathrm{Im}\Gamma_s(k) \approx -\frac{m}{4\hbar^2}[\mathrm{Re}\Gamma_s(k)]^2, \tag{24}$$

where

$$\begin{aligned}\Gamma_s(k) \approx \Gamma_s^{(1)}(k) &= -\frac{2\pi\hbar^2}{m}gkl\,[\mathbf{L}_{-1}(2kl) - \mathrm{I}_1(2kl)] \\ &\approx -\frac{2\pi\hbar^2}{m}gkl\frac{4}{\pi}\left(1-\frac{\pi}{2}kl\right)\end{aligned} \tag{25}$$

is just angular average of Eq. (14). In Eq. (25), $\mathbf{L}_n(z)$ and $\mathrm{I}_n(z)$ are the modified Struve and Bessel functions, respectively, and the Taylor expansion in powers of kl gives a good approximation for $kl \lesssim 0.2$.

V. THE MANY-BODY PROBLEM

Coming back to the many-body problem, we note that the amplitude of the interlayer scattering in all three regimes is negative in the s-wave channel (in regime C this requires $E \sim \varepsilon_F \gg E_b$, which is realistic in the limit $g \ll 1$). This means that at sufficiently low temperatures, the bilayer fermionic dipolar system undergoes a BCS pairing transition into a superfluid state with interlayer s-wave Cooper pairs, characterized by an order parameter $\Delta(\mathbf{p}) \sim \langle\hat{\psi}_-(\mathbf{p})\hat{\psi}_+(-\mathbf{p})\rangle$ with $\hat{\psi}_\alpha(\mathbf{p})$ being the field operator in the momentum space, which is independent of the azimuthal angle φ, $\Delta(\mathbf{p}) = \Delta(p)$.

A. BCS approach to pairing

The critical temperature T_c of this transition is calculated from the linearized gap equation. In the simplest BCS approach, which does not take into account many-body effects (see below), this equation for the considered system is (in what follows we will use the wavevector $\mathbf{k}$ instead of the momentum $\mathbf{p}$)

$$\Delta(\mathbf{k}) = -\int\frac{d\mathbf{k}'}{(2\pi)^2}\tilde{V}_{2D}(\mathbf{k}-\mathbf{k}')\frac{\tanh(\xi_{k'}/2T_c)}{2\xi_{k'}}\Delta(\mathbf{k}'), \tag{26}$$

where $\xi_k = \hbar^2k^2/2m - \mu = \hbar^2(k^2-k_F^2)/2m$ and $\tilde{V}_{2D}(\mathbf{k}-\mathbf{k}')$ is given explicitly by Eq. (8). In the regime $k_Fl \gtrsim 1$, this equation can be solved directly. For a dilute gas ($k_Fl < 1$), however, the gap equation (26) with the bare interparticle interaction $\tilde{V}_{2D}(\mathbf{k})$ is not convenient because it mixes many-body physics (BCS pairing) with the two-body one (scattering). In a dilute gas, they are well separated in momentum space: The pairing originates from the momenta on the order of the Fermi momenta, $p \sim p_F$, while the two-particle scattering is related to high momenta $p \sim \hbar/l \gg p_F$ that correspond to short interparticle distances, at which the presence of other particles is irrelevant and physics is described by the two-particle Schrödinger equation. For the pairing problem, the two-body physics can be taken into account by expressing the bare interparticle interaction $\tilde{V}_{2D}(\mathbf{p}-\mathbf{p}')$ in terms of the scattering amplitude $\Gamma(E,\mathbf{k},\mathbf{k}')$ using Eq. (12). This results in the renormalized (linearized) gap equation

$$\begin{aligned}\Delta(\mathbf{k}) = -\int &\frac{d\mathbf{k}'}{(2\pi\hbar)^2}\Gamma(2\mu,\mathbf{k},\mathbf{k}') \\ &\times\left[\frac{\tanh(\xi_{k'}/2T_c)}{2\xi_{k'}} + \frac{1}{2\mu - \hbar^2k'^2/m + i0}\right]\Delta(\mathbf{k}'),\end{aligned} \tag{27}$$

where we make the natural choice $E = 2\mu$. The contribution to the integral in this equation comes only from momenta $p = \hbar k' \sim p_F$, and, therefore, the form (27) of the gap equation is more suitable to describe the BCS pairing in a many-body dilute system.

In the regime of weak coupling characterized by a small parameter $\lambda = \nu_F\Gamma \ll 1$, where $\nu_F = m/2\pi\hbar^2$ is the density of state on the Fermi surface ($k = k' = k_F$), this equation can be solved by expanding in powers of λ (see below) or numerically. However, the linearized BCS gap equation (27) can be used only for the calculation of the leading contribution to the critical temperature, corresponding to the terms $\sim\lambda^{-1}$ in the exponent. As was shown by Gor'kov and Melik-Barkhudarov [25], the terms of order unity in the exponent affecting the preexponential factor in the expression for the critical temperature are determined by the next-to-leading-order terms, which depend on many-body effects. In the considered fermionic dipolar system, these effects result in the appearance of the effective mass m_* and the effective interparticle interaction. The latter corresponds to the interactions between particles in a many-body system through the polarization of the medium: virtual creation of particle-hole pairs. The BCS pairing with the account of the many-body effects can be viewed as a pairing of quasiparticles of mass m_* interacting with the effective interaction V_{eff}. Note that, in contrast to the Fermi gas with a short-range interaction, in which the difference between the bare m and the effective m_* masses (or, in other words, between particles and quasiparticles) are of the second order in λ, in the dipolar system this difference is typically of the first order in λ due to the momentum dependence of the dipolar interactions.

B. The role of many-body effects

Qualitatively the role of the many-body effects in the gap equation can be understood as follows. After performing the integration over momenta, the gap equation can be qualitatively written as

$$1 = \nu_F^* V_{\mathrm{eff}}\left(\ln\frac{\mu}{T_c} + C\right), \tag{28}$$

where $\nu_F^* = m_*/2\pi\hbar^2$ is the density of states of quasiparticles with the effective mass m_*, and we replace the scattering amplitude Γ with some effective interaction $V_{\rm eff} = \Gamma + \delta V$ with δV being the many-body contribution to the interparticle interaction. Note that the (large) logarithm $\ln \mu/T_c$ results from the integration over momenta near the Fermi surface, whereas the momenta far from the Fermi surface contribute to the constant $C \sim 1$. We can now expand $\nu_F^* V_{\rm eff}$ in powers of λ up to the second-order term, $\nu_F^* V_{\rm eff} = \lambda + a\lambda^2$, where the first term results from the direct interparticle interaction and the many-body effects (the difference between m_* and m together with δV) contribute to the second term. In solving Eq. (28) iteratively, we notice that $\lambda \ln \mu/T_c \sim 1$, and, therefore, the terms $a\lambda^2 \ln \mu/T_c$ and λC are of the same order. As a result, both terms have to be taken into account for the calculation of the critical temperature. It is easy to see that they contribute to the preexponential factor in the expression for the critical temperature. These contributions are usually called Gor'kov-Melik-Barkhudarov (GM) corrections [25]. It is important to notice that the many-body effects appear in Eq. (28) only in combination with the logarithm $\ln \mu/T_c$ that originates from momenta near the Fermi surface. Therefore, it is sufficient for our purposes to consider the many-body contributions only at the Fermi surface, and the renormalized linearized gap equation with the account of the many-body effects reads

$$\Delta(\mathbf{k}) = -\frac{m_*}{m}\int \frac{d\mathbf{k}'}{(2\pi)^2}\Gamma(2\mu,\mathbf{k},\mathbf{k}') \times \left[\frac{\tanh(\xi_{k'}/2T_c)}{2\xi_{k'}} + \frac{1}{2\mu - \hbar^2 k'^2/m + i0}\right]\Delta(\mathbf{k}') - \int_{k'<\Lambda k_F}\frac{d\mathbf{k}'}{(2\pi)^2}\delta V(\mathbf{k},\mathbf{k}')\frac{\tanh(\xi_{k'}/2T_c)}{2\xi_{k'}}\Delta(\mathbf{k}'), \tag{29}$$

where we introduce an upper cutoff Λk_F with $\Lambda \sim 1$ for the purpose of the convergency at large momenta. As discussed above, the exact value of Λ is not important because the large momenta contribution to this integral has to be neglected.

1. *Effective mass*

The contribution to the effective mass originates from the momentum and frequency dependencies of the self-energy $\Sigma_\alpha(\omega,p)$ of fermions (see, for example, Ref. [26]), $m/m_* = (1 + 2m\partial\Sigma/\partial p^2)(1 - \partial\Sigma/\partial\omega)^{-1}|_{p=p_F,\omega=0}$. In the considered case, the leading contributions to the self-energy are shown in Fig. 3, where the fermionic Green's function is

$$G_\alpha(\omega,p) = \frac{1}{\omega - \xi_p + i0\,\mathrm{sgn}(\xi_p)}.$$

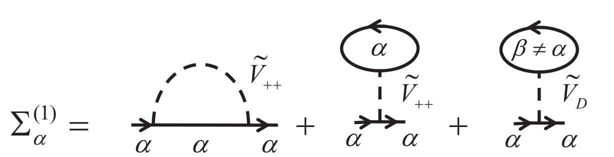

FIG. 3. The first-order diagrams for the fermionic self-energy. Dashed lines correspond to the dipole-dipole interactions. The first two diagrams contain only the intralayer interaction, while the last one describes the effects of the interlayer coupling.

It is easy to see that $\Sigma_\alpha^{(1)}(\omega,p)$ is frequency independent, $\Sigma_\alpha^{(1)}(\omega,p) = \Sigma_\alpha(p)$, and the momentum dependence results only from the first diagram, which corresponds to the exchange intralayer interaction (the momentum-independent part of the self-energy leads to unessential change of the chemical potential). The analytical expression for $\Sigma_\alpha^{(1)}(p)$ reads ($p = \hbar k$)

$$\Sigma_\alpha^{(1)}(p) = -\int\frac{d\mathbf{q}}{(2\pi)^2}[\tilde V_{++}(\mathbf{k}-\mathbf{q}) - \tilde V_{++}(\mathbf{0})]N(q) + \tilde V_{2D}(0)n = -\int\frac{d\mathbf{q}}{(2\pi)^2}[\tilde V_{++}(\mathbf{k}-\mathbf{q}) - \tilde V_{++}(\mathbf{0})]N(q),$$

where $N(q) = \theta(k_F - q)$ is the Fermi-Dirac distribution for zero temperature (the usage of n_q at zero temperature is justified by the exponential smallness of the critical temperature T_c) and $\tilde V_{+-}(\mathbf{k})$ is the Fourier transform of $\tilde V_{++}(\boldsymbol{\rho})$, and straightforward calculations with the usage of Eqs. (5) and (6) give (see, for example, Ref. [27])

$$\frac{m_*}{m} = 1 - \frac{4}{3\pi}a_d k_F = 1 - \frac{4}{3\pi}g k_F l. \tag{30}$$

It is easy to see that higher-order contribution will introduce small parameters $gk_F l_0$ or $gk_F l$ and, therefore, can be neglected.

2. *Effective interparticle interaction*

Let us now discuss the many-body contributions to the effective interparticle interaction. We consider first the case when the scattering of two particles with energies on the order of the Fermi energy corresponds to regime A ($g < k_F l < 1$), and, hence, is well controlled by the Born expansion in powers of the bare interparticle interaction with the small parameter $\lambda = \nu_F\Gamma \sim gk_F l$. As was argued above, it is sufficient to consider only the lowest (second order in the interparticle interactions) many-body contributions to the effective interaction. These contributions are shown in Fig. 4, and the corresponding analytical expressions read

$$\delta V_a(\mathbf{k},\mathbf{k}') = 2\int\frac{d\mathbf{q}}{(2\pi)^2}\frac{N(\mathbf{q}+\mathbf{k}_-/2) - N(\mathbf{q}-\mathbf{k}_-/2)}{\xi_{\mathbf{q}+\mathbf{k}_-/2} - \xi_{\mathbf{q}-\mathbf{k}_-/2}} \times \tilde V_{2D}(\mathbf{k}_-)\tilde V'_{++}(\mathbf{k}_-), \tag{31}$$

$$\delta V_b(\mathbf{k},\mathbf{k}') = -\int\frac{d\mathbf{q}}{(2\pi)^2}\frac{N(\mathbf{q}+\mathbf{k}_-/2) - N(\mathbf{q}-\mathbf{k}_-/2)}{\xi_{\mathbf{q}+\mathbf{k}_-/2} - \xi_{\mathbf{q}-\mathbf{k}_-/2}} \times \tilde V_{2D}(\mathbf{k}_-)\tilde V'_{++}(\mathbf{q}-\mathbf{k}_+/2), \tag{32}$$

$$\delta V_c(\mathbf{k},\mathbf{k}') = -\int\frac{d\mathbf{q}}{(2\pi)^2}\frac{N(\mathbf{q}+\mathbf{k}_-/2) - N(\mathbf{q}-\mathbf{k}_-/2)}{\xi_{\mathbf{q}+\mathbf{k}_-/2} - \xi_{\mathbf{q}-\mathbf{k}_-/2}} \times \tilde V_{2D}(\mathbf{k}_-)\tilde V'_{++}(\mathbf{q}+\mathbf{k}_+/2), \tag{33}$$

$$\delta V_d(\mathbf{k},\mathbf{k}') = -\int\frac{d\mathbf{q}}{(2\pi)^2}\frac{N(\mathbf{q}+\mathbf{k}_+/2) - N(\mathbf{q}-\mathbf{k}_+/2)}{\xi_{\mathbf{q}+\mathbf{k}_+/2} - \xi_{\mathbf{q}-\mathbf{k}_+/2}} \times \tilde V_{2D}(\mathbf{q}-\mathbf{k}_-/2)\tilde V_{2D}(\mathbf{q}+\mathbf{k}_-/2), \tag{34}$$

where $\mathbf{k}_\pm = \mathbf{k}\pm\mathbf{k}'$ and we keep only the momentum-dependent part $\tilde V'_{++}$ of the intralayer potential because the contributions of the momentum-independent part of $\tilde V_{++}$ in

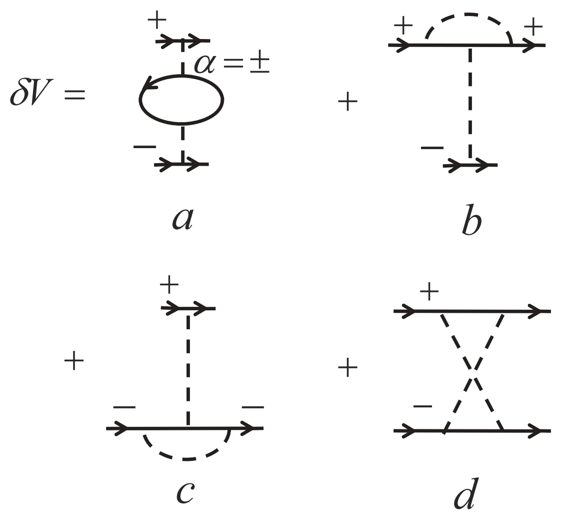

FIG. 4. The second-order contributions to the effective interlayer interaction. Solid lines correspond to particles from different layers (labeled by + and −), and the dashed lines correspond to dipole-dipole interactions. Note that panel (d) contains only the interlayer interaction, while panels (a), (b), and (c) have both the inter- and intralayer interactions.

δV_a, δV_b, and δV_c cancel each other, as they should. The contribution $\delta V_a(\mathbf{k},\mathbf{k}')$ can be calculated analytically: For $k = k' = k_F$ we have $k_- \leqslant 2k_F$ and, hence,

$$\begin{aligned}\delta V_a(\mathbf{k},\mathbf{k}') &= -2\nu_F \tilde{V}_{2D}(\mathbf{k}_-)\tilde{V}'_{++}(\mathbf{k}_-)\\ &\approx -\frac{m}{\pi\hbar^2}\left(-\frac{2\pi\hbar^2}{m}g|\mathbf{k}-\mathbf{k}'|l\right)^2\\ &= -\frac{4\pi\hbar^2}{m}(gl)^2(\mathbf{k}-\mathbf{k}')^2,\end{aligned}$$

while the other three can be computed numerically. The corresponding s-wave contributions are obtained by averaging over the directions of $\mathbf{k}$ and $\mathbf{k}'$ (azimuthal angles φ and φ', respectively):

$$\overline{\delta V_i} = \langle \delta V_i(\mathbf{k},\mathbf{k}')\rangle_{\varphi,\varphi'} \equiv \int_0^{2\pi} \frac{d\varphi d\varphi'}{(2\pi)^2}\delta V_i(\mathbf{k},\mathbf{k}'), \quad i = a,b,c,d.$$

The contribution $\overline{\delta V_i}$ can be written in the form

$$\overline{\delta V_i} = \frac{2\pi\hbar^2}{m}(gk_F l)^2 \eta_a,$$

where $\eta_a = -4$ and numerical calculation of the integrals for $\delta V_b = \delta V_c$ and δV_d result in

$$\eta_b = \eta_c = 1.148, \quad \eta_d = 0.963.$$

As a result we obtain

$$\overline{\delta V} = \frac{2\pi\hbar^2}{m}(gk_F l)^2 \sum_i \eta_i = -0.741\frac{2\pi\hbar^2}{m}(gk_F l)^2. \tag{35}$$

In regime B ($\exp(-1/g^2) \ll k_F l < g < 1$) the leading contribution to the two-particle interlayer scattering is given by the second-order Born term, and the small parameter of the theory characterizing the interlayer scattering is $\lambda = \nu_F \Gamma = -g^2/4$. For the intralayer scattering, however, the leading contribution is still given by the first-order Born term $\sim gk_F l$. This is because the intralayer scattering occurs between identical fermions, and, hence, the dominant contribution is the p-wave one. The second-order Born contribution in this case is proportional to $(gk_F l)^2 \ln(k_F l_0)$ (see Ref. [28]) or $(gk_F l)^2 \ln(gk_F l)$ for $l_0 \to 0$ (see Ref. [29]) and can be neglected. As a result, the leading contributions to the effective interparticle interaction will be given by the same diagram from Fig. 4, in which all interaction $\tilde{V}_{2D}$ lines that connect fermionic lines belonging to different layers are replaced with the second-order Born scattering amplitude $\Gamma^{(2)}$. It is then easy to see that the contribution to $\delta V(\mathbf{k},\mathbf{k}')$ comes from Fig. 4(d) and equals ($k = k' = k_F$)

$$\delta V(\mathbf{k},\mathbf{k}') \approx \nu_F \left[-\frac{2\pi\hbar^2}{m}\frac{g^2}{4}\right]^2 = \frac{2\pi\hbar^2}{m}\left[\frac{g^2}{4}\right]^2 = \nu_F^{-1}\lambda^2. \tag{36}$$

The interlayer scattering amplitude in regime C [$\exp(-1/g^2) \lesssim kl \ll g < 1$] is $\Gamma(E,\mathbf{k},\mathbf{k}') \approx (4\pi\hbar^2/m)[\ln(E_b/E) + i\pi]^{-1} \approx (4\pi\hbar^2/m)\ln^{-1}(E_b/E)$, similar to the scattering amplitude for a short-range potential. The corresponding small parameter is simply $\lambda = 2/\ln(E_b/\varepsilon_F)$. (Note the conditions Re$\lambda < 0$ and $|\lambda| < 1$ require $\varepsilon_F > E_b$.) Arguments, similar to those given for regime B, lead us to the conclusion that the leading many-body contribution to the effective interparticle interaction is given in Fig. 4(d), in which the interaction lines are replaced with the scattering amplitude (see analogous considerations in Ref. [30]):

$$\delta V(\mathbf{k},\mathbf{k}') \approx \frac{2\pi\hbar^2}{m}\frac{4}{\ln^2(E_b/\varepsilon_F)} = \nu_F^{-1}\lambda^2. \tag{37}$$

Note that the leading many-body contribution to the effective interparticle interaction in regimes B and C can be written as

$$\delta V(\mathbf{k},\mathbf{k}') = \nu_F^{-1}\lambda^2, \tag{38}$$

which is independent on the directions of $\mathbf{k}$ and $\mathbf{k}'$ and, hence, coincides with its s-wave component, $\overline{\delta V} = \nu_F^{-1}\lambda^2$.

VI. CRITICAL TEMPERATURE IN THE DILUTE LIMIT

We now proceed with the solution of the gap equation (29) in the dilute limit $kl < 1$. As we have already pointed out, the order parameter has the s-wave symmetry, $\Delta(\mathbf{k}) = \Delta(k)$, and, therefore, it is convenient to work with the gap equation projected to the s-wave channel:

$$\begin{aligned}\Delta(k) = &-\frac{m_*}{m}\int_0^\infty \frac{k'dk'}{2\pi}\Gamma_s(2\mu,k,k')\\ &\times\left[\frac{\tanh(\xi_{k'}/2T_c)}{2\xi_{k'}} + \frac{1}{2\mu - \hbar^2k'^2/m + i0}\right]\Delta(k')\\ &-\int_0^{\Lambda k_F}\frac{k'dk'}{2\pi}\overline{\delta V}\frac{\tanh(\xi_{k'}/2T_c)}{2\xi_{k'}}\Delta(k'),\end{aligned} \tag{39}$$

where $\Gamma_s(2\mu,k,k')$ is the s-wave component of the vertex function for the interlayer scattering [see Eq. (22)].

Note that following our previous discussion, the combination $(m_*/m)\Gamma_s(2\mu,k,k')$ in Eq. (39) has to be calculated to second order in the small parameter, and the second-order term has to be taken at the Fermi surface ($k = k' = k_F$), similar to the $\overline{\delta V}$ contribution. All these second-order terms can be treated perturbatively.

A. BCS approach

In the first order in the small parameter Eq. (39) corresponds to the BCS gap equation

$$\Delta(k) = -\int_0^\infty \frac{k'dk'}{2\pi}\Gamma_s(2\mu,k,k') \times \left[\frac{\tanh(\xi_{k'}/2T_c)}{2\xi_{k'}} + \frac{1}{2\mu - \hbar^2k'^2/m + i0}\right]\Delta(k'). \tag{40}$$

In order to solve this equation, we rewrite it in the form

$$\Delta(\xi) = -\int_{-\mu}^\infty d\xi' R(\xi,\xi')\left[\frac{\tanh(\xi_{k'}/2T_c)}{2\xi_{k'}} - \frac{1}{2\xi_{k'} - i0}\right]\Delta(\xi'), \tag{41}$$

where $R(\xi,\xi') = \nu_F\Gamma_s(2\mu,k_\xi,k'_{\xi'})$ with $\xi = \hbar^2k^2/2m - \mu$, $k_\xi = \hbar^{-1}\sqrt{2m(\xi+\mu)}$, and $k'_{\xi'} = \hbar^{-1}\sqrt{2m(\xi'+\mu)}$.

We then introduce a characteristic energy ω, which is on the order of the Fermi energy, and, on the other hand, is much larger than the critical temperature, $\omega \gg T_c$, and divide the integral over ξ' in Eq. (41) into three parts: (a) the integration of $R(\xi,0)\Delta(0)$ from $-\omega$ to ω, (b) the integration of $R(\xi,\xi')\Delta(\xi') - R(\xi,0)\Delta(0)$ from $-\omega$ to ω, and (c) the integration of $R(\xi,\xi')\Delta(\xi')$ from $-\mu$ to $-\omega$ and from ω to ∞. In part (a) we use the asymptotic formula

$$\int_{-\omega}^{\omega} d\xi' \frac{\tanh(\xi_{k'}/2T_c)}{2\xi_{k'}} \approx \ln\frac{2\exp(\gamma)\omega}{\pi T_c},$$

while in parts (b) and (c) we replace $\tanh(\xi_{k'}/2T_c)$ by the step function (omitting the unimportant contribution from a narrow interval $|\xi'| \lesssim T_c \ll \omega$) and integrate by parts. Equation (41) then takes the form

$$\begin{aligned}\Delta(\xi) = &-\left[\ln\frac{2\exp(\gamma)\omega}{\pi T_c} - i\frac{\pi}{2}\right]R(\xi,0)\Delta(0) \\ &- \ln\frac{\mu}{\omega}R(\xi,-\mu)\Delta(-\mu) \\ &- \int_{-\mu}^0 d\xi' \ln\left|\frac{\xi'}{\omega}\right|\frac{d}{d\xi'}[R(\xi,\xi')\Delta(\xi')],\end{aligned} \tag{42}$$

where the first term comes from part (a).

It is easy to see that the first term is larger than the second and the third ones by a factor $\ln[2\exp(\gamma)\omega/\pi T_c]$, and, therefore, the last two terms contribute only to the preexponential factor in the expression for the critical temperature. In order to solve Eq. (42), we choose ω such that

$$\ln\frac{\mu}{\omega}R(0,-\mu)\Delta(-\mu) + \int_{-\mu}^0 d\xi'\ln\left|\frac{\xi'}{\omega}\right|\frac{d}{d\xi'}[R(0,\xi')\Delta(\xi')] = 0, \tag{43}$$

and, putting $\xi = 0$ in Eq. (42), we obtain the following equation to find the critical temperature:

$$\Delta(0) = -\left[\ln\frac{2\exp(\gamma)\omega}{\pi T_c} - i\frac{\pi}{2}\right]R(0,0)\Delta(0). \tag{44}$$

It follows from this equation that

$$\ln\frac{2\exp(\gamma)\omega}{\pi T_c} - i\frac{\pi}{2} = -\frac{1}{R(0,0)}, \tag{45}$$

and, therefore, after using Eq. (24),

$$T_c^{\rm BCS} = \frac{2\exp(\gamma)}{\pi}\omega\exp\left[\frac{1}{R'(0,0)}\right], \tag{46}$$

where R' is the real part of R, $R' = \mathrm{Re}R$, such that $R = R' + iR''$, and $R'' \approx -(\pi/2)(R')^2$, according to Eq. (24).

The value of the energy ω can be obtained from Eq. (43):

$$\begin{aligned}\ln\omega &= \ln\mu\frac{R(0,-\mu)\Delta(-\mu)}{R(0,0)\Delta(0)} + \frac{1}{R(0,0)\Delta(0)} \\ &\quad\times\int_{-\mu}^0 d\xi'\ln|\xi'|\frac{d}{d\xi'}[R(0,\xi')\Delta(\xi')] \\ &= \ln\mu + \frac{1}{R(0,0)\Delta(0)}\int_{-\mu}^0 d\xi'\ln\frac{|\xi'|}{\mu} \\ &\quad\times\frac{d}{d\xi'}[R(0,\xi')\Delta(\xi')].\end{aligned} \tag{47}$$

Substituting Eqs. (45) and (50) into Eq. (42) results in the equation for the order parameter

$$\Delta(\xi) = \frac{R(\xi,0)}{R(0,0)}\Delta(0) + \int_{-\mu}^0 d\xi'\ln\left|\frac{\xi'}{\mu}\right| \times\frac{d}{d\xi'}\left\{\left[\frac{R(\xi,0)}{R(0,0)}R(0,\xi') - R(\xi,\xi')\right]\Delta(\xi')\right\}, \tag{48}$$

in which the second term is proportional to the small parameter and, hence, can be considered as a perturbation. Therefore, to leading order in the small parameter, the solution of Eq. (48) reads

$$\Delta(\xi) \approx \frac{R(\xi,0)}{R(0,0)}\Delta(0). \tag{49}$$

Substituting this expression into Eq. (47), we obtain

$$\ln\omega = \ln\mu + \frac{1}{R(0,0)^2}\int_{-\mu}^0 d\xi'\ln\frac{|\xi'|}{\mu}\frac{d}{d\xi'}[R(0,\xi')R(\xi',0)], \tag{50}$$

where we can replace all functions R with their real parts R' [see Eq. (24)]. This expression, together with Eq. (46), provides the answer for the critical temperature in the BCS approach.

B. Critical temperature in the many-body system

Following our previous discussion, one should take into account only those many-body contributions that appear in combination with the large logarithm $\ln(\varepsilon_F/T_c)$ originating from the momenta close to the Fermi momenta. Therefore, in view of the many-body contributions, Eq. (44) can be written as

$$\begin{aligned}\Delta(0) = &-\frac{m_*}{m}\left[\ln\frac{2e^\gamma\omega}{\pi T_c} - i\frac{\pi}{2}\right]R(0,0)\Delta(0) \\ &- \ln\frac{2e^\gamma\omega}{\pi T_c}\nu_F\overline{\delta V}\Delta(0) \\ \approx &-\left[\frac{m_*}{m}R(0,0) + \nu_F\overline{\delta V}\right]\left[\ln\frac{2e^\gamma\omega}{\pi T_c} - i\frac{\pi}{2}\right]\Delta(0).\end{aligned}$$

Therefor,e

$$\begin{aligned}\ln\frac{2e^{\gamma}\omega}{\pi T_c}-i\frac{\pi}{2}&\\ &=-\frac{1}{m_*R(0,0)/m+\nu_F\overline{\delta V}}\\ &\approx-\frac{1}{m_*R'(0,0)/m+iR''(0,0)+\nu_F\overline{\delta V}}\\ &\approx-\frac{1}{R'(0,0)}+\frac{\left(\frac{m_*}{m}-1\right)R'(0,0)+\nu_F\overline{\delta V}+iR''(0,0)}{R'(0,0)^2}\\ &\approx-\frac{1}{R'(0,0)}+\frac{1}{R'(0,0)}\left(\frac{m_*}{m}-1\right)+\frac{\nu_F\overline{\delta V}}{R'(0,0)^2}-i\frac{\pi}{2}.\end{aligned}$$

As a result, for the critical temperature we obtain

$$\begin{aligned}T_c&=\frac{2e^{\gamma}\omega e^{1/R'(0,0)}}{\pi}\exp\left[-\frac{m_*/m-1}{R'(0,0)}-\frac{\nu_F\overline{\delta V}}{R'(0,0)^2}\right]\\ &=T_c^{\rm BCS}\exp\left[-\frac{m_*/m-1}{R'(0,0)}-\frac{\nu_F\overline{\delta V}}{R'(0,0)^2}\right],\end{aligned}\tag{51}$$

where ω and m_* are given by Eqs. (50) and (30), respectively. The specific expression for the many-body contribution to the effective interparticle interaction $\overline{\delta V}$ depends on the regime of scattering [see Eqs. (35), (36), and (37)].

We now analyze the expression (51) for the critical temperature for different scattering regimes:

Regime A. For $g<k_Fl<1$, we have

$$\begin{aligned}R'(0,0)&\approx\nu_F\Gamma_s^{(1)}(k_F)\\ &\quad-\frac{g^2}{4}\{1-2(k_Fl)^2[5.4+3\ln(k_Fl)]\}-\frac{4g^3}{15}\\ &\approx-gk_Fl\frac{4}{\pi}\left(1-\frac{\pi}{2}k_Fl\right)\\ &\quad-\frac{g^2}{4}\{1-2(k_Fl)^2\,[5.4+3\ln(k_Fl)]\}-\frac{4g^3}{15},\end{aligned}\tag{52}$$

$$\frac{m_*}{m}-1\approx-\frac{4}{3\pi}gk_Fl,\tag{53}$$

$$\nu_F\overline{\delta V}\approx-0.741(gk_Fl)^2,\tag{54}$$

where we expand $\nu_F\Gamma_s^{(1)}(k_F)$ in the expression for $R'(0,0)$ up to the second order in powers of k_Fl, and keep only those terms that give contributions up to order unity in the expression for the critical temperature. For the calculation of ω [see Eq. (50)], it is sufficient to take $R(0,0)$ in the form $R(0,0)=\nu_F\langle\tilde V_{2D}(\mathbf{k}-\mathbf{k}')\rangle_{\varphi,\varphi'}$. The resulting integration can be performed in the same way as for the integral I_2 from Appendix D, and we obtain

$$\omega=\mu\exp\left[-0.697\left(\frac{\pi}{4}\right)^2\right]=0.651\mu.$$

With the help of Eqs. (52)–(54) we can write (within the accepted accuracy)

$$\begin{aligned}\frac{1}{R'(0,0)}&\approx-\left[\nu_F\left|\Gamma_s^{(1)}(k_F)\right|+\frac{g^2}{4}+\frac{4g^3}{15}\right]^{-1}\\ &\quad-\frac{1}{2}\left(\frac{\pi}{4}\right)^2[5.4+3\ln(k_Fl)]\\ &\approx-\left[gk_Fl\frac{4}{\pi}\left(1-\frac{\pi}{2}k_Fl\right)+\frac{g^2}{4}+\frac{4g^3}{15}\right]^{-1}\\ &\quad-1.17-0.925\ln(k_Fl),\end{aligned}\tag{55, 56}$$

$$\frac{m_*/m-1}{R'(0,0)}\approx\frac{1}{3},$$

$$\frac{\nu_F\overline{\delta V}}{[R'(0,0)]^2}\approx-0.741\left(\frac{\pi}{4}\right)^2=-0.457.$$

From Eq. (51) we now obtain the final expression for the critical temperature for the BCS pairing in regime A of interparticle scattering:

$$\begin{aligned}T_{c,a}&=\frac{2e^{\gamma}}{\pi}0.651\mu\exp\Bigg\{-\left[\nu_F\left|\Gamma_s^{(1)}(k_F)\right|+\frac{g^2}{4}+\frac{4g^3}{15}\right]^{-1}\\ &\quad-1.17-0.925\ln(k_Fl)+\frac{-1}{3}+0.457\Bigg\}\\ &\approx0.259\mu(k_Fl)^{-0.925}\\ &\quad\times\exp\left\{-\left[gk_Fl\left(\frac{4}{\pi}-\frac{k_Fl}{2}\right)+\frac{g^2}{4}+\frac{4g^3}{15}\right]^{-1}\right\},\end{aligned}\tag{57}$$

where for $k_Fl\lesssim0.2$ one has $\nu_F\Gamma_s^{(1)}(k_F)\approx gk_Fl\frac{4}{\pi}(1-\frac{\pi}{2}k_Fl)$. The comparison of this result with the one obtained in Ref. [12] in the BCS approach shows that the many-body effects result in a larger (by a factor of two) numerical prefactor. This is the effect of the competition of decreasing of the critical temperature because of the smaller effective mass and increasing T_c because of the attractive many-body contribution to the interparticle interaction. In addition, Eq. (57) contains an extra term $4g^3/15$ in the denominator in the exponent, originating from the third-order contribution in the particle-scattering amplitude. This term is smaller than the other two. However, one needs a stronger condition, namely, $g<(k_Fl)^{3/2}$, to neglect this term. This is because being expanded, this results in the contribution $\sim g^3/(k_Fl)^3=(g/k_Fl)^2(k_Fl)^{-1}$, which is small only under the stronger condition. Note that this term also leads to the higher critical temperature in the BCS approach.

The order parameter [Eq. (49)] in this regime has the form ($k'=k_F$)

$$\begin{aligned}\Delta(k)&\sim g\langle|\mathbf{k}-\mathbf{k}'|l\exp(-|\mathbf{k}-\mathbf{k}'|l)\rangle_{\varphi,\varphi'}+\frac{g^2}{4}\\ &\approx g\langle|\mathbf{k}-\mathbf{k}'|l(1-|\mathbf{k}-\mathbf{k}'|l)\rangle_{\varphi,\varphi'}+\frac{g^2}{4}\\ &=g\left\{\frac{2}{\pi}(k+k_F)l\;E\left[\frac{4kk_F}{(k+k_F)^2}\right]-\left(k^2+k_F^2\right)l^2\right\}+\frac{g^2}{4},\end{aligned}$$

where $E(z)$ is the complete elliptic integral, and we assume $kl,k_Fl\lesssim0.2$ to ensure the reasonable accuracy of the truncated expansion.

Regime B. In regime B, $k_Fl<g<1$, we have

$$\begin{aligned}R'(0,0)&\approx-\frac{g^2}{4}-gk_Fl\frac{4}{\pi}\left(1-\frac{\pi}{2}k_Fl\right)-\frac{4g^3}{15}\\ &\quad-\frac{g^4}{32}\left[\ln(4\hbar^2/m\mu l^2)+\frac{7}{2}-2\gamma\right],\end{aligned}$$

$$\approx \frac{2}{\ln(E_b/\mu)} - gk_F l \frac{4}{\pi}\left(1 - \frac{\pi}{2}k_F l\right), \tag{58}$$

$$\frac{m_*}{m} - 1 \approx -\frac{4}{3\pi} gk_F l, \tag{59}$$

$$\nu_F \overline{\delta V} \approx \left[\frac{g^2}{4}\right]^2. \tag{60}$$

The leading-order contribution in $R'(0,0)$ is momentum and energy independent, and, therefore, we have $\omega = \mu$. From Eqs. (58)–(60) we obtain

$$\frac{1}{R'(0,0)} \approx -\left[\frac{g^2}{4} + gk_F l \frac{4}{\pi}\left(1 - \frac{\pi}{2}k_F l\right) + \frac{4g^3}{15}\right]^{-1} + \frac{1}{2}\left[\ln\left(\frac{4\hbar^2}{m\mu l^2}\right) + \frac{7}{2} - 2\gamma\right],$$

$$\frac{m_\star/m - 1}{R'(0,0)} \approx \frac{14}{3\pi}\frac{k_F l}{g} \ll 1, \qquad \frac{\nu_F \overline{\delta V}}{[R'(0,0)]^2} \approx 1. \tag{61}$$

Note that the many-body contribution to the effective mass is negligible because the leading term in the scattering amplitude is momentum and energy independent. From Eq. (51) we then obtain

$$\begin{aligned} T_{c,b} &= \frac{2e^\gamma}{\pi}\mu \exp\left\{-\left[\frac{g^2}{4} + gk_F l \frac{4}{\pi}\left(1 - \frac{\pi}{2}k_F l\right) + \frac{4g^3}{15}\right]^{-1} + \frac{1}{2}\left[\ln\left(\frac{4\hbar^2}{m\mu l^2}\right) + \frac{7}{2} - 2\gamma\right] - 1\right\} \\ &= \frac{4e^{3/4}}{\pi}\sqrt{\frac{\mu\hbar^2}{ml^2}} \times \exp\left\{-\left[\frac{g^2}{4} + gk_F l\left(\frac{4}{\pi} - 2k_F l\right) + \frac{4g^3}{15}\right]^{-1}\right\} \\ &= 2.7\sqrt{\frac{\mu\hbar^2}{ml^2}} \times \exp\left[-\frac{1}{g^2/4 + 4gk_F l/\pi - 2gk_F^2 l^2 + 4g^3/15}\right]. \end{aligned} \tag{62}$$

Furthermore, we note that the exponent in this expression coincides with that in Eq. (57), and, following the same arguments as in Eq. (57), we keep some higher terms in the denominator in the exponent.

Regime C. Finally, for $\exp(-1/g^2) \lesssim k_F l \ll g < 1$,

$$R'(0,0) \approx \frac{2}{\ln(E_b/\mu)}, \quad \frac{m_*}{m} - 1 \approx \frac{4}{3\pi} gk_F l \ll 1, \qquad \nu_F \overline{\delta V} \approx \left[\frac{2}{\ln(E_b/\mu)}\right]^2,$$

where E_b is given by Eq. (11). Therefore, taking into account that, similar to regime B, $\omega = \mu$, we obtain

$$\begin{aligned} T_{c,c} &= \frac{2e^\gamma}{\pi}\mu \exp\left[\frac{1}{2}\ln(E_b/\mu) - 1\right] \\ &= \frac{2\exp(\gamma - 1)}{\pi}\sqrt{\mu E_b} = 0.42\sqrt{\mu E_b}. \end{aligned} \tag{63}$$

This expression is completely analogous to the critical temperature in a two-component 2D Fermi gas with a short-range interparticle interaction (see Ref. [30]), as it should be in this regime.

Note that within the accepted accuracy, both expressions (62) and (63) for the critical temperature in regimes B and C can be written in the form

$$\begin{aligned} T_{c,bc} &= \frac{2e^\gamma}{\pi e}\mu \exp\left\{\left[\frac{2}{\ln(E_b/\mu)} - \frac{gk_F l}{\pi/4}\left(1 - \frac{k_F l}{2/\pi}\right)\right]^{-1}\right\} \\ &= 0.42\mu \exp\left\{\left[\frac{2}{\ln(E_b/\mu)} - gk_F l\frac{4}{\pi}\left(1 - \frac{\pi}{2}k_F l\right)\right]^{-1}\right\}. \end{aligned} \tag{64}$$

In both these regimes, the order parameter is to the leading-order momentum independent, $\Delta(k) \sim$ const.

Equations (57) and (64) provide the answer for the critical temperature of the BCS transition in a dilute bilayer dipolar gas. The corresponding values of T_c calculated according to these formulas are small, $T_c \lesssim 10^{-3}$–$10^{-2}\mu$, because the exponent in Eqs. (57) and (64) contains the inverse of the product (or square) of the small parameters of the problem. For example, even for $k_F l = 0.5$ and $g = 0.45 < k_F l$, one has $T_c \approx 10^{-2}\mu$. This makes an experimental realization of the superfluid state very challenging. The situation is more promising in the dense case.

VII. CRITICAL TEMPERATURE IN THE DENSE LIMIT

We assume now that $k_F l \gtrsim 1$ and $g \ll 1$ such that $gk_F l = k_F a_d < 1$(and $k_F l_0 \ll 1$). The condition $gk_F l < 1$ ensures the validity of the perturbative expansion in powers of the interlayer interaction, although the mean interparticle interaction is comparable or larger that the range of the potential l. For this reason there is no need to renormalize the gap equation: Two colliding particles are no more well separated from the rest of the system, but many-particles collisions are still well controlled by the small parameter $a_d k_F = gk_F l < 1$. With the account of the many-body effects, the gap equation for the pairing in the s-wave channel reads

$$\Delta(k) = -\frac{m_*}{m}\int_0^\infty \frac{k'dk'}{2\pi} V_{\mathrm{eff},s}(k,k')\frac{\tanh(\xi_{k'}/2T_c)}{2\xi_{k'}}\Delta(k'), \tag{65}$$

where $V_{\mathrm{eff},s}(k,k')$ is the effective interparticle interaction in the s-wave channel,

$$\begin{aligned} V_{\mathrm{eff},s}(k,k') &= \langle \tilde{V}_{2D}(\mathbf{k} - \mathbf{k}') + \delta V(\mathbf{k},\mathbf{k}')\rangle_{\varphi,\varphi'} \\ &= \Gamma_s^{(1)}(k,k') + \langle \delta V(\mathbf{k},\mathbf{k}')\rangle_{\varphi,\varphi'}. \end{aligned}$$

Here

$$\Gamma_s^{(1)}(k,k') = \langle \tilde{V}_{2D}(\mathbf{k} - \mathbf{k}')\rangle_{\varphi,\varphi'}$$

and, as before, all many-body corrections have to be taken at the Fermi surface (assuming $T_c \ll \mu$). Using the same arguments as in the previous section, we can argue that the critical temperature T_c is related to the critical temperature in the BCS approach $T_c^{\rm BCS}$ (with no many-body contributions) as

$$T_c = T_c^{\rm BCS} \exp\left[-\frac{m_*/m - 1}{R'(0,0)} - \frac{\nu_F \overline{\delta V}}{[R'(0,0)]^2}\right], \quad (66)$$

where $R'(0,0) = \nu_F \Gamma_s^{(1)}(k_F,k_F)$ and $T_c^{\rm BCS}$ is determined by the BCS gap equation

$$\Delta(k) = -\int_0^\infty \frac{k'dk'}{2\pi}\langle \tilde{V}_{2D}(\mathbf{k}-\mathbf{k}')\rangle_{\varphi,\varphi'} \frac{\tanh\left(\xi_{k'}/2T_c^{\rm BCS}\right)}{2\xi_{k'}}\Delta(k')$$
$$= -\int_0^\infty \frac{k'dk'}{2\pi}\Gamma_s^{(1)}(k,k')\frac{\tanh\left(\xi_{k'}/2T_c^{\rm BCS}\right)}{2\xi_{k'}}\Delta(k'). \quad (67)$$

The solution of this equation is actually given by Eqs. (46) and (50): Although we are dealing with the nonrenormalized gap equation, the renormalization can still be performed as a formal trick. [Note that within the accepted accuracy, $R'(0,0)$ in Eq. (46) has to be calculated up to the second Born approximation, while only up to the first order in Eq. (50).] Nevertheless, we give here an alternative solution of the gap equation that follows the lines of Ref. [31] and avoid the renormalization.

A. BCS approach

We rewrite Eq. (67) in the form

$$\Delta(\xi) = -\int_{-\mu}^\infty d\xi' \frac{\tanh\left(\xi'/2T_c^{\rm BCS}\right)}{2\xi'}R(\xi,\xi')\Delta(\xi'), \quad (68)$$

where $\xi = \hbar^2(k^2-k_F^2)/2m$,

$$R(\xi,\xi') = \nu_F\Gamma_s^{(1)}(k,k') = gl\int_0^\pi \frac{d\varphi}{\pi}e^{-l\sqrt{k^2+k'^2-2kk'\cos\varphi}}$$
$$\times \sqrt{k^2+k'^2-2kk'\cos\varphi}, \quad (69)$$

and, following the method of Ref. [31], decompose the interaction function $R(\xi,\xi')$ into a separable part and a remainder $r(\xi,\xi')$ that vanishes when either argument is on the Fermi surface:

$$R(\xi,\xi') = R(0,0)v(\xi)v(\xi') + r(\xi,\xi') \quad (70)$$

with $v(\xi) = R(\xi,0)/R(0,0) = R(0,\xi)/R(0,0)$ and $r(\xi,0) = r(0,\xi') = 0$. Note that $v(0) = 1$ and $v(\xi)$ decays exponentially at large momenta $kl \gg 1$, i.e., $ml^2\xi/\hbar^2 \gg 1$. Equation (68) then takes the form

$$d\Delta(\xi) = -R(0,0)v(\xi)\int_{-\mu}^\infty d\xi'\frac{\tanh\left(\xi'/2T_c^{\rm BCS}\right)}{2\xi'}v(\xi')\Delta(\xi')$$
$$-\int_{-\mu}^\infty d\xi'\frac{\tanh\left(\xi'/2T_c^{\rm BCS}\right)}{2\xi'}r(\xi,\xi')\Delta(\xi'). \quad (71)$$

For $\xi = 0$ this equation reduces to

$$\Delta(0) = -R(0,0)\int_{-\mu}^\infty d\xi'\frac{\tanh\left(\xi'/2T_c^{\rm BCS}\right)}{2\xi'}v(\xi')\Delta(\xi'), \quad (72)$$

and, therefore, we can rewrite Eq. (71) as follows:

$$\Delta(\xi) = v(\xi)\Delta(0) - \int_{-\mu}^\infty d\xi'\frac{\tanh\left(\xi'/2T_c^{\rm BCS}\right)}{2\xi'}r(\xi,\xi')\Delta(\xi')$$
$$\approx v(\xi)\Delta(0) - \int_{-\mu}^\infty \frac{d\xi'}{2|\xi'|}r(\xi,\xi')\Delta(\xi'), \quad (73)$$

where we replace $\tanh(\xi'/2T_c^{\rm BCS})$ with $\mathrm{sgn}(\xi')$ assuming that $T_c \ll \mu$ and neglecting exponentially small contributions [the integral is converging because $r(\xi,0) = 0$]. In Eq. (72) we can now single out the large logarithmic contribution that comes from momenta near the Fermi surface. This can be achieved by writing $d\xi'/\xi' = d(\ln\xi')$ and integrating by part with the following result:

$$\Delta(0) = -R(0,0)\left\{\frac{1}{2}v(-\mu)\Delta(-\mu)\ln\mu - \frac{1}{2}\int_{-\mu}^\infty d\xi'\right.$$
$$\left.\times \ln|\xi'|\frac{d}{d\xi'}\left[\tanh\left(\xi'/2T_c^{\rm BCS}\right)v(\xi')\Delta(\xi')\right]\right\}.$$

After performing the derivative,

$$\frac{d}{d\xi'}\left[\tanh\left(\frac{\xi'}{2T_c^{\rm BCS}}\right)v(\xi')\Delta(\xi')\right]$$
$$= \frac{1}{2T_c^{\rm BCS}}\frac{1}{\cosh^2\left(\xi'/2T_c^{\rm BCS}\right)}v(\xi')\Delta(\xi')$$
$$+ \tanh\left(\frac{\xi'}{2T_c^{\rm BCS}}\right)\frac{d}{d\xi'}[v(\xi')\Delta(\xi')],$$

and using the fact that $1/2T_c^{\rm BCS}\cosh^2(\xi'/2T_c^{\rm BCS})$ is sharply peaked at $\xi' = 0$, we obtain

$$\Delta(0) = -R(0,0)\left\{\frac{1}{2}v(-\mu)\Delta(-\mu)\ln\mu + \ln\frac{2e^\gamma}{\pi T_c^{\rm BCS}}\Delta(0)\right.$$
$$\left.-\frac{1}{2}\int_{-\mu}^\infty d\xi'\ln|\xi'|\mathrm{sgn}(\xi')\frac{d}{d\xi'}[v(\xi')\Delta(\xi')]\right\}$$
$$= -R(0,0)\left\{\ln\frac{2\mu e^\gamma}{\pi T_c^{\rm BCS}}\Delta(0)\right.$$
$$\left.-\frac{1}{2}\int_{-\mu}^\infty d\xi'\ln\frac{|\xi'|}{\mu}\frac{d}{d|\xi'|}[v(\xi')\Delta(\xi')]\right\}, \quad (74)$$

where we again replace $\tanh(\xi'/2T_c^{\rm BCS})$ with $\mathrm{sgn}(\xi')$.

The pair of equations (74) and (73) can now be solved iteratively because the integrals in both equations provide small corrections when $k_F l \gtrsim 1$ (see below). In the leading order, we have for the order parameter $< \xi'$

$$\Delta(\xi) \approx v(\xi)\Delta(0).$$

[Note that the second iteration of Eq. (73) with the explicit expression $r(\xi,\xi') = R(\xi,\xi') - R(\xi,0)R(0,\xi')/R(0,0)$ can be rewritten in the form of Eq. (48).] From Eq. (74) we then obtain

$$T_c^{\rm BCS} = \frac{2e^\gamma}{\pi}\mu\exp\left\{-\frac{1}{2}\int_{-\mu}^\infty d\xi'\ln\frac{|\xi'|}{\mu}\frac{d}{d|\xi'|}[v(\xi')^2]\right\}$$
$$\times\exp\left[\frac{1}{R(0,0)}\right] \quad (75)$$

for the critical temperature in the BCS approach.

To establish the connection with the approach from the previous section, we notice that

$$-\frac{1}{2}\int_{-\mu}^{\infty} d\xi' \ln\frac{|\xi'|}{\mu}\frac{d}{d|\xi'|}[v(\xi')^2]$$
$$= -\frac{1}{2}\int_{-\mu}^{\infty} d\xi' \ln\frac{|\xi'|}{\mu}\frac{d}{d\xi'}[v(\xi')^2]$$
$$+\int_{-\mu}^{0} d\xi' \ln\frac{|\xi'|}{\mu}\frac{d}{d\xi'}[v(\xi')^2].$$

The last term in the right-hand side can now be identified with the contribution to $\ln\omega$ [see Eq. (50)], and the first one with the second-order Born contribution to $R'(0,0)$.

Before going further, let us discuss the conditions for the iterative approach to the system of Eqs. (74) and (73) to be legitimate. In Eq. (73), this requires that the second term is small and, hence, $\Delta(\xi)/\Delta(0) \approx v(\xi)$. For $k_F l \sim 1$, one can see that the relative contribution of the second term is on the order of $gk_F l$. Therefore, the iterative scheme with the result $\Delta(\xi) \approx v(\xi)\Delta(0)$ is legitimate for $gk_F l = a_d l < 1$. For a dilute system with $k_F l \ll 1$, the situation is more subtle. In this case, the contribution from $\xi' \lesssim \mu$ in the second term gives the relative contribution on the order of $gk_F l$, while the regime $\mu < \xi' \lesssim \hbar^2/ml^2$ results in the relative contribution $\sim g/k_F l$. Therefore, for $g < k_F l$ both contributions are small, and the iterative procedure is legitimate. However, for the opposite case $g > k_F l$, the contribution from the second region is large, and the iterative scheme breaks down. The reason for this is the large value of $r(\xi,\xi')$ for $\xi' \gg \mu$. The proper iterative procedure in this case can be developed on the basis of the renormalized gap equation.

B. Critical temperature in the many-body system

The calculation of the many-body contributions to the critical temperature can be performed in the same way as in the dilute regime because, although $k_F l \gtrsim 1$, we assume that $gk_F l = a_d k_F < 1$, and, hence, the expansion in powers of interparticle interaction is still valid. The corresponding contributions to the self-energy (effective mass) and interparticle interaction are shown in Figs. 3 and 4, and the analytic expressions are given by Eqs. (30) and (31)–(34), respectively. Note that $\delta V_a(\mathbf{k},\mathbf{k}')$ can be calculated analytically:

$$\delta V_a(\mathbf{k},\mathbf{k}') = -2\nu_F \tilde{V}_{2D}(\mathbf{k}-\mathbf{k}')\tilde{V}'_{++}(\mathbf{k}-\mathbf{k}')$$
$$\approx -\frac{4\pi\hbar^2}{m}(g|\mathbf{k}-\mathbf{k}'|l)^2\exp(-|\mathbf{k}-\mathbf{k}'|l),$$

[as before, we keep only the momentum-dependent part of $\tilde{V}_{++}(\mathbf{k}-\mathbf{k}')$] together with its angular average for $k = k' = k_F$,

$$\nu_F\delta\overline{V}_a = -8(gk_F l)^2\left[\mathrm{I}_0(2k_F l) - \frac{1}{2}{}_0F_1\left(2;k_F^2 l^2\right)\right.$$
$$\left.-\frac{8}{3\pi}(k_F l)_1F_2\left(2;\frac{3}{2},\frac{5}{2};k_F^2 l^2\right)\right],$$

where $\mathrm{I}_0(z)$ is the modified Bessel function and ${}_nF_m(a_1,\ldots,a_n;b_1,\ldots,b_m;z)$ is the hypergeometric function,

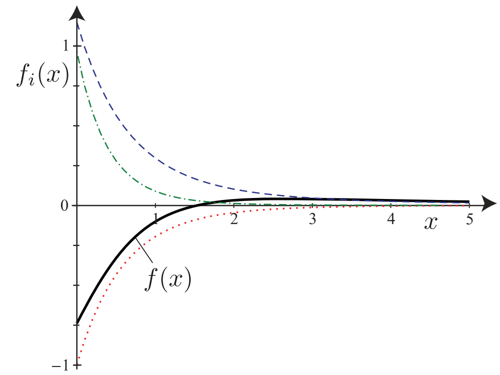

FIG. 5. (Color online) The functions $f_a(x)/4$, $f_b(x) = f_c(x)$, $f_d(x)$, and $f(x)$ (dotted, dash-dotted, dashed, and solid lines, respectively).

while the other three contributions require numerical integrations. We write these contributions as

$$\nu_F\delta\overline{V}_i = (gk_F l)^2 f_i(k_F l), \quad i = a,b,c,d,$$

where the functions $f_i(x)$ are shown in Fig. 5. The overall angular averaged contribution to the effective interaction then reads

$$\nu_F\delta\overline{V} = (gk_F l)^2 f(k_F l),$$

where the function $f(x) = f_a(x) + 2f_b(x) + f_c(x)$ is also shown in Fig. 5 (solid line).

After writing $R(0,0)$ in the form

$$R(0,0) = -\frac{4}{\pi}gk_F l\gamma(k_F l),$$

where

$$\gamma(x) = \frac{1}{2}\int_0^{\pi} d\varphi\sin(\varphi)e^{-x\sin(\varphi)} = \frac{\pi}{4}\left[\mathbf{L}_{-1}(2x) - \mathrm{I}_1(2x)\right]$$

[see Eq. (25)], which is shown in Fig. 6, we obtain

$$-\frac{1}{R(0,0)}\left(\frac{m_*}{m}-1\right) - \frac{\nu_F\delta\overline{V}}{[R(0,0)]^2}$$
$$= -\frac{1}{3\gamma(k_F l)} - \left(\frac{\pi}{4}\right)^2\frac{f(k_F l)}{\gamma(k_F l)^2}. \qquad (76)$$

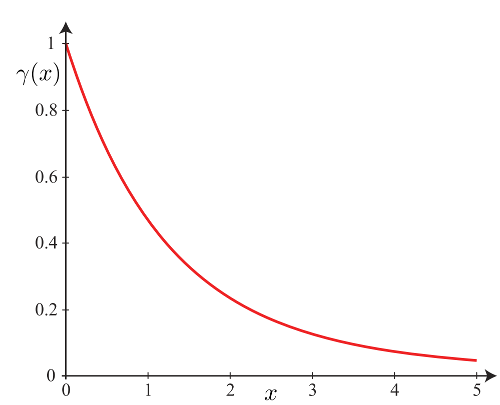

FIG. 6. (Color online) The function $\gamma(x)$.

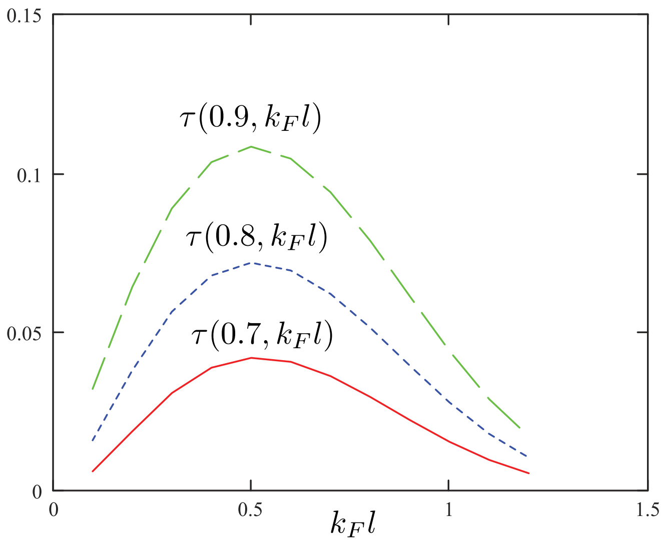

FIG. 7. (Color online) The function $\tau(g,x)$ for $g=0.7$ (solid line), $g=0.8$ (short-dashed line), and $g=0.9$ (long-dashed line).

Finally, after combining together Eqs. (75), (66), and (76), we find

$$T_c = \frac{2e^\gamma}{\pi}\mu \exp\left[-\frac{1}{16}\frac{\Omega(k_F l)}{\gamma(k_F l)^2} - \frac{1}{3\gamma(k_F l)} - \left(\frac{\pi}{4}\right)^2\frac{f(k_F l)}{\gamma(k_F l)^2}\right] \times \exp\left[-\frac{\pi}{4gk_F l}\frac{1}{\gamma(k_F l)}\right], \tag{77}$$

where

$$\Omega(x) = \frac{1}{2}\int_0^\infty ds \ln|1-s^2|\mathrm{sgn}(s-1)\frac{d}{dx}[V(s,x)^2]$$

and

$$V(s,x) = \int_0^\pi d\varphi\sqrt{1+s^2-2s\cos\varphi}\,e^{-x\sqrt{1+s^2-2s\cos\varphi}}.$$

The expression (77) is appropriate for $k_F l \gtrsim 1$. Based on the discussion after Eq. (75), we can write the expression for the critical temperature that interpolates between two regimes $k_F l \gtrsim 1$ and $k_F l \lesssim 1$:

$$\begin{aligned} T_c &= \frac{2e^\gamma}{\pi}\mu \exp\left[-\frac{1}{3\gamma(k_F l)} - \left(\frac{\pi}{4}\right)^2\frac{f(k_F l)}{\gamma(k_F l)^2}\right] \\ &\quad \times \exp\left[-\frac{\pi}{4gk_F l\gamma(k_F l)}\frac{1}{1-(4/\pi)gk_F l\gamma(k_F l)\Omega(k_F l)}\right] \\ &\equiv \frac{2e^\gamma\mu}{\pi}\tau(g,k_F l). \end{aligned} \tag{78}$$

The dependence of the function $\tau(g,k_F l)$ on $k_F l$ for several values of g is shown in Fig. 7. We see that the critical temperature decreases very rapidly for $k_F l > 1$ due to the fast decay of the scattering amplitude. The optimal value of $k_F l$ is around 0.5 with the critical temperature reaching values on the order of 0.1 μ for $g \approx 0.9$, which corresponds to $gk_F l \approx 0.45 < 1$.

VIII. CONCLUDING REMARKS

We obtain our results for the superfluid critical temperature using the mean-field approach. However, as is well known, this approach in two dimensions is applicable only at zero temperature, while at finite temperature the long-range order is destroyed by phase fluctuations, and, therefore, the mean-field order parameter is zero. In this case, the transition into the superfluid phase follows the Berezinskii-Kosterlitz-Thouless (BKT) scenario [32,33]. In the weak coupling limit, however, as was pointed out by Miyake [34], the difference between the critical temperature calculated within the mean-field approach T_c and the critical temperature of the BKT transition T_{BKT} can be estimated as $T_c - T_{\mathrm{BKT}} \sim T_c^2/\mu$ and, therefore, small as compared to T_c. As a result, our mean-field calculations provide a reliable answer for the critical temperature in the considered weak coupling regime $a_d k_F < 1$.

Let us now discuss possible physical realizations of the interlayer pairing. In the experiments with polar molecules, the values of the dipolar length a_d are on the order of 10^2–10^4 nm: For a ^{40}K^{87}Rb with currently available $d \approx 0.3$D one has $a_d \approx 170$ nm (with $a_d \approx 600$ nm for the maximum value $d \approx 0.566$ D), and for ^{6}Li^{133}Cs with a tunable dipole moment from $d = 0.35$ to 1.3 D (in an external electric field ~ 1 kV/cm), the value of a_d varies from $a_d \approx 260$ to $\approx$3500 nm. For the interlayer separation l on the order of a few hundred nanometers, the corresponding values of the parameter g can be both smaller and larger than unity ($g \lesssim 10$).

The values of the parameter $k_F l$ are also within this range for densities $n = 10^6$–10^9 cm^{-2} (for example, one has $k_F l = 1$ for $l = 500$ nm and $n \approx 3 \times 10^7$ cm^{-2}). Note, however, that the optimal values of this parameter are around $k_F l \sim 0.5$ (see Fig. 7), and, hence, the optimum value of the interlayer separation is related to the density, which, in turn, should be large enough to provide a substantial value for the Fermi energy. For ^{40}K^{87}Rb molecules at the density $n \approx 4 \times 10^8$ cm^{-2} in each layer, one has $\varepsilon_F \approx 100$ nK and $k_F \approx 7$ μm^{-1}. Therefore, the interlayer separation l should be relatively small, $l \lesssim 150$ nm, to meet the optimal conditions. For $l = 150$ nm one then has $g \approx 1.1$ (with current $d \approx 0.3$ D), $k_F l \approx 1$, and $T_c \approx 0.1\varepsilon_F \approx 10$ nK. Note that strictly speaking these values of parameters g and $k_F l$ do not correspond to the weak coupling regime considered in this paper, rather to the intermediate regime of the BCS-BEC crossover. However, based on the experience with the BEC-BCS crossover in two-component atomic fermionic mixtures (see, for example, Ref. [35]), in which the critical temperature continues to grow when approaching the crossover region from the BCS side, we could expect that the above value of the critical temperature provides a good estimate for the onset of the superfluidity in the intermediate coupling regime.

ACKNOWLEDGMENTS

We acknowledge fruitful discussions with G. Pupillo, P. Julienne, G. V. Shlyapnikov, L. Sieberer, and J. Ye. This work was supported by the Austrian Science Fund FWF (SFB FOQUS), the EU STREP NAME-QUAM, and the AFOSR MURI.

APPENDIX A: INTERLAYER BOUND STATE

We present in this Appendix some details of the calculation of the (intralayer) bound-state properties for small couplings

$g \ll 1$. Our starting point is Eq. (8), i.e., the equation for the radial wavefunction $\chi_{m_z}(\rho)$ of the bound state with binding energy E_b. Since for $g \ll 1$ one has merely one (shallow) bound state of axial symmetry, in the following we focus on the the axial symmetric case, $m_z = 0$, and derive its binding energy and wavefunction within a series in $1/g$.

On the one hand, we see from Eq. (10) that at sufficiently large distances, $\rho \gg \rho_\star$, we can neglect the interaction potential $V_{2D}(\rho)$, and the wavefunction takes the form

$$\chi_0(\rho) \approx \mathcal{C} K_0(\sqrt{mE_b}\rho/\hbar), \tag{A1}$$

with $\mathcal{C}$ a constant and $K_0(z)$ the modified Bessel function of the second kind and the distance $\rho_\star \sim (d^2/E_b)^{1/3} = (gl\hbar^2/mE_b)^{1/3} \gg l$ for $g \gg ml^2E_b/\hbar^2$. Since $\rho_\star \gg \hbar/\sqrt{mE_b} \equiv \rho_\kappa$ for $E_b \ll \hbar^2 g/ml^2$, we can expand Eq. (A1) for distances $\rho \ll \rho_k$ as

$$\chi_0(\rho) \approx \mathcal{C} \ln\left(\frac{2\hbar e^{-\gamma}}{\sqrt{mE_b}\rho}\right)$$

with $\gamma \approx 0.5772$ the Euler constant and in particular

$$\rho \frac{d}{d\rho} \ln[\chi_0(\rho)] \approx -\left[\ln\left(\frac{2\hbar}{\sqrt{mE_b}\rho}\right) - \gamma\right]^{-1}. \tag{A2}$$

On the other hand, for sufficiently small distances, $\rho \ll \rho_\star$, and weak coupling $g \ll 1$, we can neglect the bound-state energy; i.e., we assume $E_b \ll \hbar^2 g/ml^2$, and expand the wavefunction in powers of g as

$$\chi_0(\rho) \approx \mathcal{N}\left[\chi_0^{(0)}(\rho) + \sum_{n=1}^{\infty} g^n \chi_0^{(n)}(\rho)\right]$$

with $\mathcal{N}$ an overall normalization constant. Then Eq. (10) gives a set of differential equations for the various terms,

$$\frac{1}{\rho}\frac{d}{d\rho}\rho\frac{d}{d\rho}\chi_0^{(n)}(\rho) = \frac{mV_{2D}(\rho)}{\hbar^2 g}\chi_0^{(n-1)}(\rho), \tag{A3}$$

with $\chi_0^{(-1)}(\rho) \equiv 0$ and the boundary condition $\chi_0^{(n)}(0) = \delta_{n,0}$. From Eq. (A3) we obtain that the zeroth-order term is then a constant, i.e., $\chi_0^{(0)}(\rho) = 1$, while the higher-order terms are obtained by iterated integration of Eq. (A3) as

$$\chi_0^{(n)}(\rho) = \int_0^{\rho} d\rho_1 \int_0^{\rho_1} d\rho_2 \frac{\rho_2 l\left(\rho_2^2 - 2l^2\right)}{\rho_1\left(\rho_2^2 + l^2\right)^{5/2}} \chi_0^{(n-1)}(\rho_2). \tag{A4}$$

The terms up to fourth order are (with $z \equiv \sqrt{\rho^2 + l^2}/l$)

$$\chi_0^{(0)}(\rho) = 1, \quad \chi_0^{(1)}(\rho) = \frac{1}{z} - 1,$$

$$\chi_0^{(2)}(\rho) = \frac{3}{8z^2} - \frac{1}{z} + \frac{5}{8} - \frac{1}{4}\ln(z),$$

$$\chi_0^{(3)}(\rho) = \frac{3}{40z^3} - \frac{3}{8z^2} + \frac{47}{120z} - \frac{11}{120} - \frac{z-1}{4}\ln(z) - \frac{4}{15}\ln\left(\frac{z+1}{2}\right),$$

$$\chi_0^{(4)}(\rho) = \frac{3}{320z^4} - \frac{3}{40z^3} + \frac{11}{128z^2} + \frac{17}{120z} - \frac{311}{1920} + \frac{\ln^2(z)}{32} + \left(-\frac{3}{32z^2} + \frac{1}{4z} + \frac{257}{960}\right)\ln(z) + \frac{4}{15}\left(\frac{1}{z} + 1\right)\ln\left(\frac{2}{z+1}\right) + \frac{\mathrm{Li}_2(1-z^2)}{64},$$

with $\mathrm{Li}_n(z) = \sum_{k=1}^{\infty} z^k/k^n$ the polylogarithm function.

We truncate the latter expansion at order g^n and have

$$\rho\frac{d}{d\rho}\ln\chi_0(\rho) \approx \rho\frac{d}{d\rho}\ln\left[\sum_{k=0}^{n} g^k \chi_0^{(k)}(\rho)\right] \equiv \Lambda_0^{(n)}(\rho),$$

which for $\rho \gg l$ ($z \gg 1$) gives

$$\Lambda_0^{(0)}(\rho) = 0,$$

$$\Lambda_0^{(1)}(\rho) = -\frac{g}{z^2}\frac{z^2-1}{z+g(1-z)} \approx -\frac{g}{1-g}\frac{l}{\rho},$$

$$\Lambda_0^{(2)}(\rho) = \left[-\frac{4}{gz^3} + \frac{4}{gz} - \frac{3}{z^4} + \frac{4}{z^3} + \frac{2}{z^2} - \frac{4}{z} + 1\right] \times \left[-\frac{4}{g^2} - \frac{4}{gz} + \frac{4}{g} - \frac{3}{2z^2} + \frac{4}{z} + \ln(z) - \frac{5}{2}\right]^{-1} \approx \left[\ln\left(\frac{\rho}{l}\right) - \left(\frac{4}{g^2} - \frac{4}{g} + \frac{5}{2}\right)\right]^{-1},$$

$$\Lambda_0^{(3)}(\rho) \approx \left\{\ln\left(\frac{\rho}{l}\right) - \left(1 - \frac{g}{15}\right)^{-1} \times \left[\frac{4}{g^2} - \frac{4}{g} + \frac{5}{2} + \frac{32\ln(2) - 11}{30}g\right]\right\}^{-1},$$

$$\Lambda_0^{(4)}(\rho) \approx \left\{\ln\left(\frac{\rho}{l}\right) - \left(1 - \frac{g}{15} - \frac{g^2}{240}\right)^{-1} \times \left[\frac{4}{g^2} - \frac{4}{g} + \frac{5}{2} + \frac{32\ln(2) - 11}{30}g - \frac{311 + 5\pi^2 - 512\ln(2)}{480}g^2\right]\right\}^{-1}. \tag{A5}$$

Comparing the latter with the asymptotic behavior from Eq. (A2), we see that for $n \geqslant 2$ we can match their leading $\sim 1/\ln(\rho)$ behavior via the binding energy and thus obtain (up to order n), respectively,

$$\ln\left[\frac{ml^2E_b^{(2)}}{4\hbar^2 e^{-2\gamma}}\right] = -\frac{8}{g^2} + \frac{8}{g} - 5, \tag{A6a}$$

$$\ln\left[\frac{ml^2E_b^{(3)}}{4\hbar^2 e^{-2\gamma}}\right] = -\frac{8/g^2 - 8/g + 5}{1 + g/15} - \frac{32\ln(2) - 11}{15/g + 1} \approx -\frac{8}{g^2} + \frac{128}{15g} - \frac{1253}{225} + O(g), \tag{A6b}$$

$$\ln\left[\frac{ml^2E_b^{(4)}}{4\hbar^2 e^{-2\gamma}}\right] = -\frac{8/g^2 - 8/g + 5 - 11g/15 - 311g^2/240}{1 + g/15 - g^2/240} - \frac{32g(g+1)\ln(2)/15 - \pi^2 g^2/48}{1 + g/15 - g^2/240} \approx -\frac{8}{g^2} + \frac{128}{15g} - \frac{2521}{450} + O(g). \tag{A6c}$$

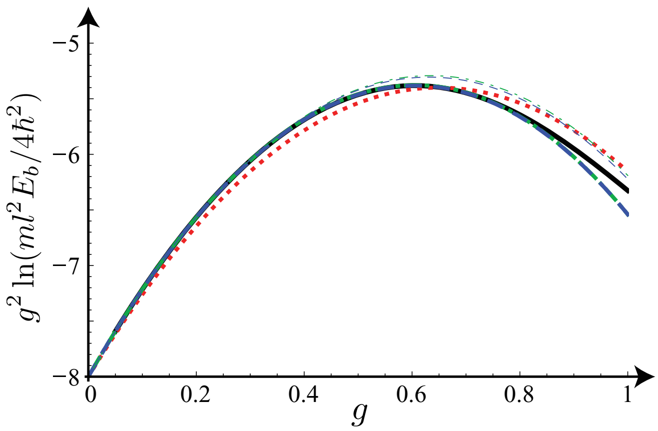

FIG. 8. (Color online) Binding energy (scaled), $g^2 \ln(ml^2E_b/4\hbar^2)$, as a function of the coupling g. Shown are the numerical result E_b^{n} (solid line) and the analytical results $E_b^{(n)}$ in $n = 2,3,4$-th-order perturbation theory (dotted, dot-dashed, dashed lines), as well as the expansion up to $O(g)$ for $n = 3,4$ (thin dot-dashed, thin dashed lines) from Eq. (A6). Note that the numerical results for $n = 3$ and 4 with this scale are practically indistinguishable. See, however, Fig. 9.

We see that the truncation at order n yields the correct expansion for the logarithm of the energy up to $O(g^{n-1})$, and thereby from the latter obtain

$$E_b \approx \frac{4\hbar^2}{ml^2} \exp\left[-\frac{8}{g^2} + \frac{128}{15g} - \frac{2521}{450} - 2\gamma + O(g)\right].$$

Concluding, we compare the analytic results for the binding energy of Eq. (A6), $E_b^{(n)}$, with the result obtain by numerical integration of the Schrödinger equation (10), E_b^{n}, which are shown in Figs. 8 and 9 .

APPENDIX B: LOW-ENERGY SCATTERING

In the following we discuss the connection of the bound state and in particular its binding energy E_b with the scattering amplitude at (very) low energy for weak coupling $g \ll 1$. Our starting is the scattering wavefunction $\psi_k^{(+)}(\boldsymbol{\rho})$ at energy $E = \hbar k^2/m$ of Sec. III.

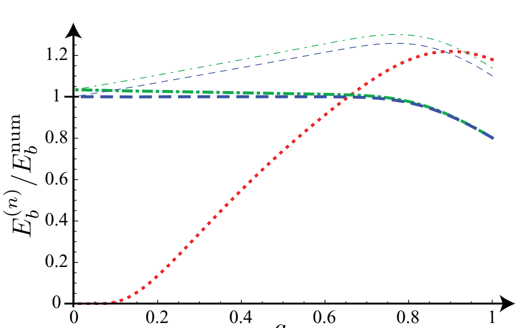

FIG. 9. (Color online) Deviation of the analytical results from the numerical result for the binding energy, $E_b^{(n)}/E_b^{\mathrm{n}}$, as a function of the coupling g for $n = 2, 3, 4$ (dotted, dot-dashed, dashed lines). Also shown is the expansion up to $O(g)$ for $n = 3, 4$ (thin dot-dashed, thin dashed lines) from Eq. (A6).

On the one hand, for $\rho \gg \rho_\star$ it takes the asymptotic form

$$\psi_k^{(+)}(\boldsymbol{\rho}) \approx \exp(i\mathbf{k}\boldsymbol{\rho}) - \frac{if_k}{4} H_0^{(1)}(k\rho),$$

with f_k the scattering amplitude and $H_0^{(1)}(z)$ the Hankel function. In the regime $k\rho_\star \ll 1$ we can further expand $\psi_k^{(+)}(\boldsymbol{\rho})$ for $\rho \ll 1/k$ as

$$\psi_k^{(+)}(\boldsymbol{\rho}) \approx 1 + \frac{f_k}{2\pi}\left[\ln\left(\frac{k\rho}{2}\right) + \gamma - \frac{i\pi}{2}\right]. \tag{B1}$$

On the other hand, for $\rho \ll \rho_\star$ and weak coupling $g \ll 1$ we can neglect the energy, i.e., take $E \to 0$, and expand the wavefunction as a power series in g as

$$\psi_k^{(+)} \approx \mathcal{N}\left[\sum_{n=0}^{\infty} g^n \chi_0^{(n)}(\rho)\right], \tag{B2}$$

where $\mathcal{N}$ is a normalization constant. The individual terms, $\chi_0^{(n)}(\rho)$, are normalized as $\chi_0^{(n)}(0) = \delta_{n,0}$ and are derived in Appendix A up to order $n = 4$ [see Eq. (A6)]. For $\rho \gg l$ (but still $\rho \ll \rho_\star$) the wavefunction approaches

$$\begin{aligned}\psi_k^{(+)}(\boldsymbol{\rho}) \approx \mathcal{N}\Bigg\{&1 - g + g^2\left[\frac{5}{8} - \frac{\ln(\rho/l)}{4}\right] \\ &+ g^3\left[\frac{4\ln(2)}{15} - \frac{11}{120} - \frac{\ln(\rho/l)}{60}\right] \\ &- g^4\left[\frac{311}{1920} + \frac{\pi^2}{384} - \frac{4\ln(2)}{15} - \frac{\ln(\rho/l)}{960}\right]\Bigg\},\end{aligned} \tag{B3}$$

which has the form of Eq. (B1), and thus we can match the two asymptotic forms. This is conveniently done in terms of the log derivative of the wavefunction as

$$\rho\frac{\partial}{\partial\rho}\ln[\psi_k^{(+)}(\boldsymbol{\rho})] \approx \left[\ln\left(\frac{k\rho}{2}\right) + \gamma + \frac{2\pi}{f_k} - \frac{i\pi}{2}\right]^{-1}, \tag{B4}$$

$$\rho\frac{\partial}{\partial\rho}\ln[\psi_k^{(+)}(\boldsymbol{\rho})] \approx \left[\ln\left(\frac{\rho}{l}\right) + \frac{\Lambda(g)}{2}\right]^{-1}, \tag{B5}$$

where $\Lambda(g)$ is obtained as in Eq. (A5) as

$$\begin{aligned}\Lambda(g) &\approx \frac{-8/g^2 + 8/g - 5 + O(g)}{1 - g/15 + g^2/240 + O(g^3)} \\ &\approx -\frac{8}{g^2} + \frac{128}{15g} - \frac{2521}{450} + O(g) \approx \ln\left[\frac{ml^2E_b}{4\hbar^2e^{-2\gamma}}\right],\end{aligned}$$

which we recognize as the perturbative expansion for the binding energy. Matching Eq. (B4) and Eq. (B5), we get the scattering amplitude explicitly as

$$f_k \approx \frac{2\pi}{\ln(2/kl) - \gamma + \Lambda(g)/2 + i\pi/2} = \frac{4\pi}{\ln(E_b/E) + i\pi},$$

which recovers the universal low-energy behavior of 2D scattering. Finally, we remark that expanding the latter expression for the scattering amplitude as a power series up to fourth order in g, we obtain

$$\frac{f_k}{2\pi} \approx -\frac{g^2}{4} - \frac{4g^3}{15} - \frac{g^4}{16}\left[\ln\left(\frac{2i}{kl}\right) - \gamma + \frac{7}{4}\right]. \tag{B6}$$

APPENDIX C: BORN SERIES FOR THE *s*-WAVE SCATTERING

In the following we derive the (s-wave) scattering amplitude within a Born expansion. We recall the relation of the s-wave scattering amplitude f_k in terms of the vertex function $\Gamma(E,\mathbf{k},\mathbf{k}')$ from Eq. (12),

$$f_k = \int \frac{d\varphi}{2\pi} f_k(\varphi) = \frac{\langle \Gamma(E,\mathbf{k},\mathbf{k}')\rangle_{\varphi,\varphi'}}{\hbar^2/m} = \frac{m}{\hbar^2}\sum_{n=1}^{\infty}\Gamma_s^{(n)}(k),$$

with $\mathbf{k},\mathbf{k}'$ on the mass shell, i.e., $k = k' = \sqrt{mE/\hbar^2}$; the averaging is performed over their azimuthal angles φ and φ', and the contributions $\Gamma_s^{(n)}(k)$ follow from the Born expansion of the vertex function $\Gamma(E,\mathbf{k},\mathbf{k}')$ [see Eq. (13)].

For convenience we introduce the s-wave potential

$$\begin{aligned}\tilde{V}_s(q_1,q_2) &= \langle \tilde{V}_{2\mathrm{D}}(\mathbf{q}_1-\mathbf{q}_2)\rangle_{\varphi_1,\varphi_2} = \langle \tilde{V}_{2\mathrm{D}}(\mathbf{q}_1-\mathbf{q}_2)\rangle_{\varphi_1}\\ &= \int \frac{d\varphi}{2\pi}\tilde{V}_{2\mathrm{D}}\left(\sqrt{q_1^2+q_2^2-2q_1q_2\cos\varphi}\right)\\ &= g\frac{2\pi\hbar^2}{m}l\frac{\partial}{\partial l}\int\frac{d\varphi}{2\pi}e^{-l\sqrt{q_1^2+q_2^2-2q_1q_2\cos\varphi}}, \end{aligned} \quad \text{(C1)}$$

which in particular for $q_1 = 0$ (or $q_2 = 0$) gives

$$\tilde{V}_s(q,0) = \tilde{V}_s(0,q) = \tilde{V}_{2\mathrm{D}}(q) = -g\frac{2\pi\hbar^2}{m}e^{-ql}ql, \quad \text{(C2)}$$

while for equal momenta, $q_1 = q_2 = q$, it gives

$$\tilde{V}_s(q,q) = -\tfrac{2\pi\hbar^2 g}{m}2ql\,[\mathbf{L}_{-1}(2ql) - I_1(2ql)], \quad \text{(C3)}$$

with $\mathbf{L}_n(z)$ the modified Struve function and $I_n(z)$ a modified Bessel function of the first kind.

The first-order contribution then explicitly gives

$$\begin{aligned}\Gamma_s^{(1)}(k) &= \langle V_{2D}(\mathbf{k}-\mathbf{k}')\rangle_{\varphi_1,\varphi_2} = \tilde{V}_s(k,k)\\ &= -\frac{2\pi\hbar^2 g}{m}2kl\,[\mathbf{L}_{-1}(2ql) - I_1(2ql)], \end{aligned}\quad \text{(C4)}$$

which vanishes for $k \to 0$, is negative for $k > 0$ with its minimum of $\approx -0.3136 \times 2\pi\hbar^2 g/m$ at $k \approx 0.7131/l$ (see Fig. 10, solid line), and for low momenta, $k \ll 1/l$, gives

$$\Gamma_s^{(1)}(k) \approx -\frac{2\pi\hbar^2 g}{m}\left[\frac{4kl}{\pi} - 2(kl)^2 + O(k^3)\right]. \quad \text{(C5)}$$

The second-order contribution to s-wave scattering is

$$\begin{aligned}\Gamma_s^{(2)}(k) &= \int\frac{d\mathbf{q}}{(2\pi)^2}\frac{\langle \tilde{V}_{2D}(\mathbf{k}-\mathbf{q})\tilde{V}_{2D}(\mathbf{q}-\mathbf{k}')\rangle_{\varphi,\varphi'}}{E-\hbar^2q^2/m+i0^+}\\ &= ⨍ \frac{qdq}{2\pi}\frac{\tilde{V}_s(k,q)\tilde{V}_s(q,k)}{E-\hbar^2q^2/m} - i\frac{m}{4\hbar^2}\tilde{V}_s(k,k)^2. \end{aligned}\quad \text{(C6)}$$

The real part, the principal value integral, in general has to be evaluated numerically and is shown in Fig. 10(a) (dashed line). We remark that it has two extrema, $\approx -0.2603 \times 2\pi\hbar^2 g^2/m$ at $k \approx 0.1364/l$ and $\approx 0.0103 \times 2\pi\hbar^2 g^2/m$ at $k \approx 2.1137/l$. Moreover for small momenta, $k \ll 1/l$, the leading contribution is

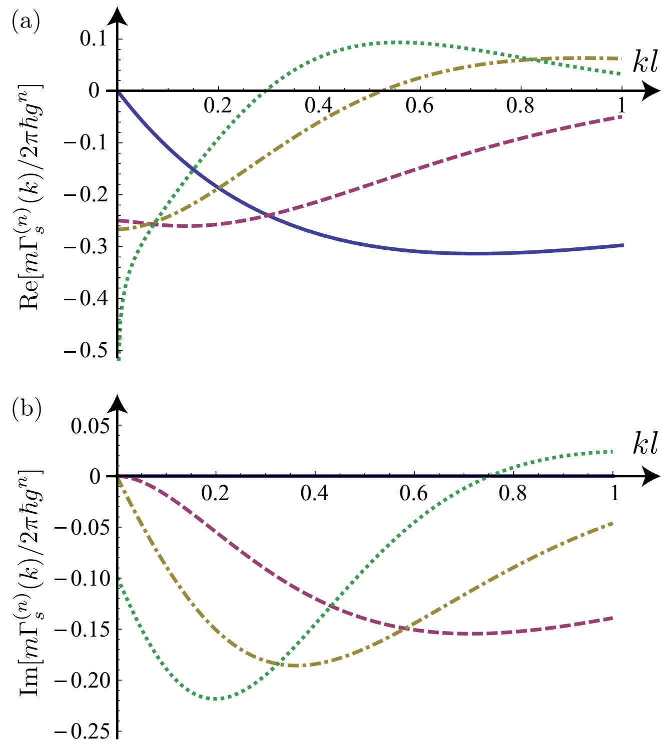

FIG. 10. (Color online) Born series for the s-wave scattering amplitude. Shown are (a) the real and (b) imaginary parts of the contributions $\Gamma_s^{(n)}(k)$ of order $n = 1, 2, 3, 4$ (solid, dashed, dash-dotted, dotted lines) as a function of momentum k.

$$\begin{aligned}\mathrm{Re}\left[\Gamma_s^{(2)}(k)\right] &\approx -\frac{2\pi\hbar^2 g^2}{m}l^2\int_0^\infty qdqe^{-2ql} + O(k)\\ &= -\frac{2\pi\hbar^2 g^2}{m}\frac{1}{4} + O(k), \end{aligned}\quad \text{(C7)}$$

which in particular is finite and negative for $k = 0$. For the imaginary part we have explicitly

$$\begin{aligned}\mathrm{Im}\left[\Gamma_s^{(2)}(k)\right] &= -\frac{m}{4\hbar^2}\tilde{V}_s(k,k)^2\\ &= -\frac{2\pi\hbar^2}{m}g^2(kl)^2 2\pi\,[\mathbf{L}_{-1}(2ql) - I_1(2ql)]^2, \end{aligned}\quad \text{(C8)}$$

with a minimum of $\approx -0.1544 \times 2\pi\hbar^2 g^2/m$ at $k \approx 0.7131/l$, see Fig. 10(b) (dashed line), and for small momenta, $k \ll 1/l$, vanishes as

$$\mathrm{Im}\left[\Gamma_s^{(2)}(k)\right] \approx -\frac{16\hbar^2}{m}g^2(kl)^2 + O(k^3). \quad \text{(C9)}$$

The third-order contribution to s-wave scattering is conveniently split into its real and imaginary parts as

$$\Gamma_s^{(3)}(k) = \int\frac{d\mathbf{q}_1 d\mathbf{q}_2}{(2\pi)^4} \times \frac{\langle \tilde{V}_{2\mathrm{D}}(\mathbf{k}-\mathbf{q}_1)\tilde{V}_{2\mathrm{D}}(\mathbf{q}_1-\mathbf{q}_2)\tilde{V}_{2D}(\mathbf{q}_2-\mathbf{k}')\rangle_{\varphi,\varphi'}}{(E-\hbar^2q_1^2/m+i0^+)(E-\hbar^2q_2^2/m+i0^+)}$$

$$= \int \frac{q_1 dq_1}{2\pi} \int \frac{q_2 dq_2}{2\pi} \times \frac{\tilde{V}_s(k,q_1)\tilde{V}_s(q_1,q_2)\tilde{V}_s(q_2,k)}{(E - \hbar^2 q_1^2/m + i0^+)(E - \hbar^2 q_2^2/m + i0^+)}$$
$$= \fint \frac{q_1 dq_1}{2\pi} \fint \frac{q_2 dq_2}{2\pi} \frac{\tilde{V}_s(k,q_1)\tilde{V}_s(q_1,q_2)\tilde{V}_s(q_2,k)}{(E - \hbar^2 q_1^2/m)(E - \hbar^2 q_2^2/m)} - \frac{\tilde{V}_s(k,k)^3}{16\hbar^4/m^2} - i\frac{V_s(k,k)}{2\hbar^2/m} \fint \frac{qdq}{2\pi} \frac{\tilde{V}_s(k,q)\tilde{V}_s(q,k)}{E - \hbar^2 q^2/m},$$

which are shown in Fig. 10 (dash-dotted lines). We notice that the real part has its minimum at $k = 0$, where

$$\mathrm{Re}\left[\Gamma_s^{(3)}(0)\right] = \int_0^\infty dq_1 \int_0^\infty dq_2 \frac{\tilde{V}_s(0,q_1)\tilde{V}_s(q_1,q_2)\tilde{V}_s(q_2,0)}{4\pi^2\hbar^4 q_1 q_2/m^2}$$
$$= g^2 l^2 \int_0^\infty dq_1 \int_0^\infty dq_2 e^{-q_1 l - q_2 l} \tilde{V}_s(q_1,q_2)$$
$$= 2\pi g^2 l^2 \int_0^\infty \rho d\rho \frac{V_{2D}(\rho)}{\rho^2 + l^2} = -\frac{2\pi\hbar^2 g^3}{m}\frac{4}{15},$$

where for the s-wave potential we used the representation

$$V_s(q_1,q_2) = 2\pi \int_0^\infty \rho d\rho V_{2D}(\rho) J_0(q_1\rho) J_0(q_2\rho),$$

and for the convolution of the Bessel function the relation

$$\int_0^\infty dq e^{-ql} J_0(q\rho) = \frac{1}{\sqrt{\rho^2 + l^2}},$$

and its maximum $\approx 0.0636 \times 2\pi\hbar^2 g^3/m$ at $k \approx 0.9205/l$. While the real part of $\Gamma_s^{(3)}(k)$ is finite and negative for $k = 0$, we notice that its imaginary part vanishes as

$$\mathrm{Im}\left[\Gamma_s^{(3)}(k)\right] = -\frac{m}{2\hbar^2}\tilde{V}_s(k,k)\mathrm{Re}\left[\Gamma_s^{(2)}(k)\right] \approx -\frac{2\pi\hbar^2 g^3}{m} kl + O(k^2), \tag{C10}$$

and two extrema, $\approx -0.1857 \times 2\pi\hbar^2 g^3/m$ at $k \approx 0.3623/l$ and $\approx 0.0059 \times 2\pi\hbar^2 g^3/m$ at $k \approx 1.9642/l$.

The fourth-order contribution to s-wave scattering is conveniently split into its real and imaginary parts as

$$\Gamma_s^{(4)}(k) = \int \frac{d\mathbf{q}_1 d\mathbf{q}_2 d\mathbf{q}_3}{(2\pi)^6} \frac{\langle \tilde{V}_{2D}(\mathbf{k} - \mathbf{q}_1) V_{2D}(\mathbf{q}_1 - \mathbf{q}_2) \tilde{V}_{2D}(\mathbf{q}_2 - \mathbf{q}_3) \tilde{V}_{2D}(\mathbf{q}_3 - \mathbf{k}')\rangle_{\varphi,\varphi'}}{(E - \hbar^2 q_1^2/m + i0^+)(E - \hbar^2 q_2^2/m + i0^+)(E - \hbar^2 q_3^2/m + i0^+)}$$
$$= \left(\frac{m}{2\pi\hbar^2}\right)^3 \int q_1 dq_1 \int q_2 dq_2 \int q_3 dq_3 \frac{V_s(k,q_1)V_s(q_1,q_2)V_s(q_2,q_3)V_s(q_3,k)}{(k^2 - q_1^2 + i0^+)(k^2 - q_2^2 + i0^+)(k^2 - q_3^2 + i0^+)}$$
$$= \fint \frac{q_1 dq_1}{2\pi} \fint \frac{q_2 dq_2}{2\pi} \fint \frac{q_3 dq_3}{2\pi} \frac{V_s(k,q_1)V_s(q_1,q_2)V_s(q_2,q_3)V_s(q_3,k)}{(E - \hbar^2 q_1^2/m)(E - \hbar^2 q_2^2/m)(E - \hbar^2 q_3^2/m)} - 3\left[\frac{V_s(k,k)}{4\hbar^2/m}\right]^2 \fint \frac{qdq}{2\pi} \frac{\tilde{V}_s(k,q)\tilde{V}_s(q,k)}{E - \hbar^2 q^2/m}$$
$$- 2i\frac{V_s(k,k)}{4\hbar^2/m} \fint \frac{q_1 dq_1}{2\pi} \fint \frac{q_2 dq_2}{2\pi} \frac{\tilde{V}_s(k,q_1)\tilde{V}_s(q_1,q_2)\tilde{V}_s(q_2,k)}{(E - \hbar^2 q_1^2/m)(E - \hbar^2 q_2^2/m)} - i\frac{m}{4\hbar^2}\left[\fint \frac{qdq}{2\pi} \frac{\tilde{V}_s(k,q)\tilde{V}_s(q,k)}{E - \hbar^2 q^2/m}\right]^2 + i\frac{V_s(k,k)^4}{(4\hbar^2/m)^3},$$

which are shown in Fig. 10 (dotted lines). We notice that the imaginary part of $\Gamma_s^{(4)}(k)$ in the limit $k \to 0$ is finite,

$$\mathrm{Im}\left[\Gamma_s^{(4)}(0)\right] = -\frac{m}{4\hbar^2}\left[\fint \frac{qdq}{2\pi} \frac{\tilde{V}_s(0,q)\tilde{V}_s(q,0)}{E - \hbar^2 q^2/m}\right]^2 = -\frac{m}{4\hbar^2}\left[\frac{2\pi\hbar^2}{m}\frac{g^2}{4}\right]^2 = -\frac{2\pi\hbar^2}{m}\frac{g^4\pi}{32},$$

with two extrema, $\approx -0.2184 \times 2\pi\hbar^2/m$ at $k \approx 1.0532/l$ and $\approx 0.0245 \times 2\pi\hbar^2/m$ at $k \approx 1.0532/l$. The real part of $\Gamma_s^{(4)}(k)$ diverges for $k \to 0$ as (for $k \ll 1/l$)

$$\mathrm{Re}\left[\Gamma_s^{(4)}(k)\right] \approx \left(\frac{m}{2\pi\hbar^2}\right)^3 \fint \frac{q_1 dq_1}{k^2 - q_1^2} \fint \frac{q_2 dq_2}{k^2 - q_2^2} \fint \frac{q_3 dq_3}{k^2 - q_3^2} \times \tilde{V}_s(k,q_1)\tilde{V}_s(q_1,q_2)\tilde{V}_s(q_2,q_3)\tilde{V}_s(q_3,k) + O(k^2)$$
$$\approx \left(\frac{m}{2\pi\hbar^2}\right)^3 \fint \frac{q_2 dq_2}{k^2 - q_2^2}\left[\fint \frac{dq}{q}\tilde{V}_s(0,q)\tilde{V}_s(q,q_2)\right]^2 + O(k)$$
$$= \frac{2\pi\hbar^2 g^4}{m} \fint \frac{qdq}{k^2 - q^2}\left[\fint \rho d\rho l^2 \frac{(\rho^2 - 2l^2)}{(\rho^2 + l^2)^3} J_0(q\rho)\right]^2 + O(k)$$
$$= \frac{2\pi\hbar^2 g^4}{m} \fint \frac{qdq}{k^2 - q^2}\left[\frac{ql}{2}K_1(ql) - \frac{3(ql)^2}{8}K_2(ql)\right]^2 + O(k)$$
$$\approx -\frac{2\pi\hbar^2 g^4}{m}\frac{1}{16}\left[\ln\left(\frac{2}{kl}\right) + \frac{7}{4} - \gamma\right] + O(k),$$

and has two extrema, i.e., $\approx 0.0937 \times 2\pi\hbar^2 g^4/m$ at $k \approx 0.5574/l$ and $\approx -0.0027 \times 2\pi\hbar^2 g^4/m$ at $k \approx 1.8438/l$.

Concluding, we remark that summing up the contributions up to fourth order in g, we obtain for $k \ll 1/l$,

$$\Gamma_s(k) \approx \sum_{n=1}^{4} \Gamma_s^{(n)}(k) \approx -\frac{2\pi\hbar^2}{m}\left\{\frac{g^2}{4} + \frac{4g^3}{15} + \frac{g^4}{16}\left[\ln\left(\frac{2}{kl}\right) + \frac{7}{4} - \gamma + \frac{i\pi}{2}\right] + O(k)\right\},$$

which coincides with the expansion of the scattering amplitude in terms of the binding energy up to fourth order in g from Eq. (B6).

APPENDIX D: THE s-WAVE ON-SHELL SCATTERING AMPLITUDE IN THE SECOND BORN APPROXIMATION

We present in this Appendix some details of the calculations of the s-wave on-shell scattering amplitude in the second Born approximation. Our starting expression is

$$\Gamma^{(2)}(E,\mathbf{k},\mathbf{k}') = \int \frac{d\mathbf{q}}{(2\pi)^2}\frac{\tilde{V}_{2D}(\mathbf{k}-\mathbf{q})\tilde{V}_{2D}(\mathbf{q}-\mathbf{k}')}{E - q^2\hbar^2/m + i0},$$

where $\tilde{V}_{2D}(\mathbf{k}-\mathbf{q})$ is given by Eq. (8), $k = k' = \sqrt{mE}/\hbar$, and we have to perform averaging over the direction of $\mathbf{k}$ and $\mathbf{k}'$ (azimuthal angles φ and φ', respectively)

$$\Gamma_s^{(2)}(k) = \int \frac{d\varphi}{2\pi}\int \frac{d\varphi'}{2\pi}\Gamma^{(2)}(E,\mathbf{k},\mathbf{k}')$$

in order to obtain the s-wave contribution.

The calculation of the imaginary part is simple and can be performed without the on-shell condition $k = k' = q_E$:

$$\begin{aligned}\mathrm{Im}\left[\Gamma^{(2)}(E,\mathbf{k},\mathbf{k}')\right] &= -\pi\int\frac{d\mathbf{q}}{(2\pi)^2}\tilde{V}_{2D}(\mathbf{k}-\mathbf{q})\tilde{V}_{2D}(\mathbf{q}-\mathbf{k}')\delta(E-q^2\hbar^2/m)\\ &= -\frac{m}{4\hbar^2}\int\frac{d\varphi_{\mathbf{q}}}{2\pi}\tilde{V}_{2D}(\mathbf{k}-\mathbf{q}_E)\tilde{V}_{2D}(\mathbf{q}_E-\mathbf{k}'),\end{aligned}$$

where $q_E = \sqrt{mE}/\hbar$. The s-wave contribution then is

$$\mathrm{Im}\left[\Gamma_s^{(2)}(E,\mathbf{k},\mathbf{k}')\right] = -\frac{m}{4\hbar^2}\langle\tilde{V}_{2D}(\mathbf{k}-\mathbf{q}_E)\rangle_{\varphi}\langle\tilde{V}_{2D}(\mathbf{q}_E-\mathbf{k}')\rangle_{\varphi'},$$

where

$$\begin{aligned}\langle\tilde{V}_{2D}(\mathbf{k}-\mathbf{q}_E)\rangle_{\varphi} &= \fint\frac{d\varphi}{2\pi}\tilde{V}_{2D}\left(\sqrt{k^2+q_E^2-2kq_E\cos\varphi}\right),\\ \langle\tilde{V}_{2D}(\mathbf{q}_E-\mathbf{k}')\rangle_{\varphi'} &= \int\frac{d\varphi'}{2\pi}\tilde{V}_{2D}\left(\sqrt{k'^2+q_E^2-2k'q_E\cos\varphi'}\right).\end{aligned}$$

On the mass shell $k = k' = q_E = \sqrt{mE}/\hbar$ and under the condition $kl \ll 1$, we have

$$\langle\tilde{V}_{2D}(\mathbf{k}-\mathbf{q}_E)\rangle_{\varphi} = -\frac{2\pi\hbar^2}{m}\frac{4}{\pi}gkl$$

and, therefore,

$$\mathrm{Im}\left[\Gamma_s^{(2)}(k)\right] = -\frac{2\pi\hbar^2}{m}\frac{8}{\pi}g^2(kl)^2. \tag{D1}$$

The calculation of the real part

$$\mathrm{Re}\left[\Gamma_s^{(2)}(k)\right] = \fint\frac{d\mathbf{q}}{(2\pi)^2}\frac{\langle\tilde{V}_{2D}(\mathbf{k}-\mathbf{q}_E)\rangle_{\varphi}\langle\tilde{V}_{2D}(\mathbf{q}-\mathbf{k}')\rangle_{\varphi'}}{\hbar^2(k^2-q^2)/m}, \tag{D2}$$

where $\fint$ denotes the principal value of the integral, is technically more involved. After introducing the new dimensionless integration variable $y = q/k$, Eq. (D2) reads

$$\mathrm{Re}\left[\Gamma_s^{(2)}(k)\right] = \frac{2\pi\hbar^2}{m}g^2\fint_0^{\infty}\frac{\varepsilon^2 y\,dy}{1-y^2}\langle R_1R_2e^{-\varepsilon(R_1+R_2)}\rangle_{\varphi_1\varphi_2},$$

where $\varepsilon = kl \ll 1$, $R_i = \sqrt{1+y^2-2y\cos\varphi_i}$, $\varphi_1 = \varphi$, and $\varphi_2 = \varphi'$. After integrating by part we obtain

$$\begin{aligned}\mathrm{Re}\left[\Gamma_s^{(2)}(k)\right] = \frac{2\pi\hbar^2}{m}\frac{g^2}{2}\varepsilon^2\int_0^{\infty}dy\ln(|1-y^2|)\\ \times\frac{d}{dy}\langle R_1R_2\exp[-\varepsilon(R_1+R_2)]\rangle_{\varphi_1\varphi_2},\end{aligned}$$

and the calculation of $\mathrm{Re}[\Gamma_s^{(2)}(k)]$ reduces to the calculation of the integral

$$I(\varepsilon) = \varepsilon^2\int_0^{\infty}dy\ln(|1-y^2|)\frac{d}{dy}\langle R_1R_2e^{-\varepsilon(R_1+R_2)}\rangle_{\varphi_1\varphi_2}$$

up to the terms $\sim\varepsilon^2\ln\varepsilon$.

It is convenient to split $I(\varepsilon)$ into two parts, i.e., $I(\varepsilon) = I_1(\varepsilon) + I_2(\varepsilon)$, where

$$\begin{aligned}I_1(\varepsilon) &= \varepsilon^2\int_0^{\infty}dy\ln(y^2-1)\frac{d}{dy}\langle R_1R_2e^{-\varepsilon(R_1+R_2)}\rangle_{\varphi_1\varphi_2},\\ I_2(\varepsilon) &= \varepsilon^2\int_1^{1}dy\ln(1-y^2)\frac{d}{dy}\langle R_1R_2e^{-\varepsilon(R_1+R_2)}\rangle_{\varphi_1\varphi_2}.\end{aligned}$$

Within the chosen accuracy, the second integral $I_2(\varepsilon)$ can be simplified as

$$I_1(\varepsilon) \approx \varepsilon^2\int_0^{1}dy\ln(1-y^2)\frac{d}{dy}\langle R_1R_2\rangle_{\varphi_1\varphi_2}$$

because it converges when $\varepsilon\to 0$ in the integrand. The result of averaging over angles φ_1 and φ_2 can now be expressed in terms of complete elliptic integrals $E(k)$ and $K(k)$:

$$\begin{aligned}I_2(\varepsilon) = \varepsilon^2\frac{4}{\pi^2}\int_0^1 dy\ln(1-y^2)\frac{1+y}{y}E(k)\\ \times[(y+1)E(k)+(y-1)K(k)],\end{aligned} \tag{D3}$$

where $k = 4y/(1+y)^2$. The numerical calculation of the above integral gives

$$I_2(\varepsilon) \approx -0.697\varepsilon^2. \tag{D4}$$

After differentiating with respect to y the integral $I_2(\varepsilon)$ reads:

$$\begin{aligned}I_2(\varepsilon) &= \varepsilon^2\int_1^{\infty}dy\ln(y^2-1)\left\langle\left\{\frac{y-\cos\varphi_1}{R_1/R_2}+\frac{y-\cos\varphi_2}{R_2/R_1}\right.\right.\\ &\quad\left.\left.-\varepsilon[(y-\cos\varphi_1)R_2+y-\cos\varphi_2)R_1]\right\}e^{-\varepsilon(R_1+R_2)}\right\rangle_{\varphi_1\varphi_2}\\ &= I_{2a}(\varepsilon)+I_{2b}(\varepsilon),\end{aligned} \tag{D5}$$

where we split the integral into the two contributions

$$\begin{aligned}I_{2a}(\varepsilon) &= \varepsilon^2\int_1^{\infty}dy\ln(y^2-1)\\ &\quad\times\left\langle e^{-\varepsilon(R_1+R_2)}\left[\frac{y-\cos\varphi_1}{R_1/R_2}+\frac{y-\cos\varphi_2}{R_2/R_1}\right]\right\rangle_{\varphi_1\varphi_2},\\ I_{2b}(\varepsilon) &= -\varepsilon^3\int_1^{\infty}dy\ln(y^2-1)\langle e^{-\varepsilon(R_1+R_2)}\\ &\quad\times[(y-\cos\varphi_1)R_2+R_1(y-\cos\varphi_2)]\rangle_{\varphi_1\varphi_2}.\end{aligned}$$

For $y > 1$ we can write

$$R_1 + R_2 \approx \sum_{i=1}^{2}\left[y - \cos\varphi_i + \frac{\sin^2\varphi_i}{2y}\right] + O(y^{-2}),$$

$$\times(y-\cos\varphi_1)R_2 + R_1(y-\cos\varphi_2)$$

$$\approx 2y^2 - 2y\sum_{i=1}^{2}\cos\varphi_i \qquad \text{(D6)}$$

$$+\frac{\sin^2\varphi_1+\sin^2\varphi_2+4\cos\varphi_1\cos\varphi_2}{2} + O(y^{-1}). \qquad \text{(D7)}$$

Note that the integral $I_{2b}(\varepsilon)$ is already proportional to ε^3, and, hence, the contribution of finite y ($1 \sim y \ll \varepsilon^{-1}$) will be beyond the necessary accuracy. Therefore, we should consider only the contribution of large y ($y \sim \varepsilon^{-1}$). In this case we can replace $\ln(y^2-1)$ with $2\ln y$ and use Eqs. (D6) and (D7). In the exponent $\exp[-\varepsilon(R_1+R_2)]$ we keep only $2\varepsilon y$ from the expansion for $\varepsilon(R_1+R_2)$ to ensure convergency, while we expand in $\varepsilon(\cos\varphi_1+\cos\varphi_2)$ and $(\varepsilon/2y)(\sin^2\varphi_1+\sin^2\varphi_2)$ to the second and first orders, respectively,

$$e^{-\varepsilon(R_1+R_2)}$$
$$\approx e^{-2\varepsilon y}\left[1+\varepsilon(\cos\varphi_1+\cos\varphi_2)+\frac{\varepsilon^2}{2}(\cos\varphi_1+\cos\varphi_2)^2\right)$$
$$\left.-\frac{\varepsilon}{2y}(\sin^2\varphi_1+\sin^2\varphi_2)+\cdots\right].$$

It is easy to see that higher-order terms in the above expansion, as well as the omitted terms in Eq. (D7), result in terms $\sim\varepsilon^3\ln\varepsilon$ or smaller. The integrations over y and the angles φ_1 and φ_2 are then straightforward and give

$$I_{2b}(\varepsilon) \approx -\tfrac{3}{2}+\gamma+\ln(2\varepsilon)+\varepsilon^2\left[\tfrac{7}{4}-\tfrac{1}{2}\gamma-\tfrac{1}{2}\ln(2\varepsilon)\right], \qquad \text{(D8)}$$

where $\gamma \approx 0.5772$ is the Euler constant.

The integral $I_{2a}(\varepsilon)$ can be rewritten in the form

$$I_{2a}(\varepsilon) = I_{2a1}(\varepsilon)+I_{2a2}(\varepsilon) = \varepsilon^2\int_1^\infty dy\,\ln(y^2-1)e^{-2\varepsilon y}$$
$$\times\left\langle\left[\frac{y-\cos\varphi_1}{R_1}R_2 + R_1\frac{y-\cos\varphi_2}{R_2}\right]\right\rangle_{\varphi_1\varphi_2}$$
$$+\varepsilon^2\int_1^\infty dy\,\ln(y^2-1)\Big\langle[e^{-\varepsilon(R_1+R_2)}-e^{-2\varepsilon y}]$$
$$\times\left[\frac{y-\cos\varphi_1}{R_1/R_2}+\frac{y-\cos\varphi_2}{R_2/R_1}\right]\Big\rangle_{\varphi_1\varphi_2}. \qquad \text{(D9)}$$

In the second integral, $I_{2a2}(\varepsilon)$, we can write [cf. Eq. (D6)]

$$e^{-\varepsilon(R_1+R_2)}-e^{-2\varepsilon y}$$
$$\approx \varepsilon e^{-2\varepsilon y}\left[\cos\varphi_1+\cos\varphi_2+\frac{\varepsilon}{2}(\cos\varphi_1+\cos\varphi_2)^2\right.$$
$$\left.-\frac{\sin^2\varphi_1+\sin^2\varphi_2}{2y}+\cdots\right],$$

$$\frac{y-\cos\varphi_1}{R_1/R_2}+\frac{y-\cos\varphi_2}{R_2/R_1}$$
$$\approx 2y-(\cos\varphi_1+\cos\varphi_2)+\frac{\cos\varphi_1+\cos\varphi_2}{2y^2}$$
$$\times(\cos\varphi_1-\cos\varphi_2)^2+\cdots. \qquad \text{(D10)}$$

The calculations are now similar to those that led us to Eq. (D8), and we obtain

$$\varepsilon^2\int_1^\infty dy\,\ln(y^2-1)\Big\langle\left[\frac{y-\cos\varphi_1}{R_1/R_2}+\frac{y-\cos\varphi_2}{R_2/R_1}\right]$$
$$\times[e^{-\varepsilon(R_1+R_2)}-e^{2\varepsilon y}]\Big\rangle_{\varphi_1\varphi_2} \approx \frac{\varepsilon^2}{2}[1-3\gamma+3\ln(2\varepsilon)].$$

In order to calculate the first integral, $I_{2a1}(\varepsilon)$, in Eq. (D9), we notice that for $y \gg 1$

$$\left\langle\left[\frac{y-\cos\varphi_1}{R_1/R_2}+\frac{y-\cos\varphi_2}{R_2/R_1}\right]\right\rangle_{\varphi_1\varphi_2} \approx 2y-\frac{3}{16y^3}+\cdots,$$

$$\ln(y^2-1)\approx 2\ln y-\frac{1}{y^2}+\mathrm{O}(y^{-3}),$$

and rewrite $I_{2a1}(\varepsilon)$ as follows:

$$\varepsilon^2\int_1^\infty dy\,\ln(y^2-1)e^{-2\varepsilon y}\left\langle\left[\frac{y-\cos\varphi_1}{R_1/R_2}+\frac{y-\cos\varphi_2}{R_2/R_1}\right]\right\rangle_{\varphi_1\varphi_2}$$
$$=\varepsilon^2\int_1^\infty dy\left[2\ln y-\frac{1}{y^2}\right]2ye^{-2\varepsilon y}$$
$$+\varepsilon^2\int_1^\infty dy\left[\ln(y^2-1)-2\ln y+\frac{1}{y^2}\right]2ye^{-2\varepsilon y}$$
$$+\varepsilon^2\int_1^\infty dy\,\ln(y^2-1)e^{-2\varepsilon y}$$
$$\times\left\langle\left[\frac{y-\cos\varphi_1}{R_1/R_2}+\frac{y-\cos\varphi_2}{R_2/R_1}\right]-2y\right\rangle_{\varphi_1\varphi_2}.$$

The second and the third integrals in the right-hand-site of this equation converge at $y \sim 1$, and, therefore, we can replace $e^{-2\varepsilon y}$ with unity. As a result we obtain

$$\varepsilon^2\int_1^\infty dy\,\ln(y^2-1)e^{-2\varepsilon y}\left\langle\left[\frac{y-\cos\varphi_1}{R_1/R_2}+\frac{y-\cos\varphi_2}{R_2/R_1}\right]\right\rangle_{\varphi_1\varphi_2}$$
$$=\varepsilon^2\int_1^\infty dy\left[2\ln y-\frac{1}{y^2}\right]2y\exp(-2\varepsilon y)$$
$$+\varepsilon^2\int_1^\infty dy\left[\ln(y^2-1)-2\ln y+\frac{1}{y^2}\right]2y+\varepsilon^2\int_1^\infty dy$$
$$\times\ln(y^2-1)\left\langle\left[\frac{y-\cos\varphi_1}{R_1/R_2}+\frac{y-\cos\varphi_2}{R_2/R_1}\right]-2y\right\rangle_{\varphi_1\varphi_2}. \qquad \text{(D11)}$$

The integrations over y and angles φ_1 and φ_2 are then straightforward, and we obtain

$$\varepsilon^2\int_1^\infty dy\,\ln(y^2-1)e^{-2\varepsilon y}\left\langle\left[\frac{y-\cos\varphi_1}{R_1/R_2}+\frac{y-\cos\varphi_2}{R_2/R_1}\right]\right\rangle_{\varphi_1\varphi_2}$$
$$=1-\gamma-\ln(2\varepsilon)+\varepsilon^2[1+2\gamma+2\ln(2\varepsilon)]-\varepsilon^2$$
$$+2\varepsilon^2\int_1^\infty dy\,\ln(1-y^2)\Big(\frac{2}{\pi^2}\frac{1+y}{y}E(k)[(y+1)E(k)$$
$$+(y-1)K(k)]-y\Big)$$

$$\approx 1-\gamma-\ln(2\varepsilon)+\varepsilon^2\Bigg\{2\gamma+2\ln(2\varepsilon)+2\int_1^\infty dy \times \ln(1-y^2)\bigg(\frac{2}{\pi^2}\frac{1+y}{y}E(k)[(y+1)E(k) +(y-1)K(k)]-y\bigg)\Bigg\},$$

where again $k=4y/(1+y)^2$. Numerical evaluation of the remaining integral gives

$$2\int_1^\infty dy\,\ln(y^2-1)\bigg\{\frac{2}{\pi^2}\frac{1+y}{y}E(k)[(y+1)E(k) +(y-1)K(k)]-y\bigg\}\approx 0.0384, \tag{D12}$$

and, hence,

$$I_{2a2}(\varepsilon)\approx 1-\gamma-\ln(2\varepsilon)+2\varepsilon^2[\gamma+\ln(2\varepsilon)+0.0192] +\tfrac{1}{2}\varepsilon^2[1-5\gamma-5\ln(2\varepsilon)] = 1-\gamma-\ln(2\varepsilon)+\varepsilon^2[2\gamma+2\ln(2\varepsilon)+0.03834]. \tag{D13}$$

Combining together Eqs. (D4), (D13), and (D8), we get

$$I(\varepsilon)=-\tfrac{1}{2}+\varepsilon^2\,[3.323+3\ln(2\varepsilon)]\,,$$

and, as a result,

$$\mathrm{Re}\big[\Gamma_s^{(2)}(k)\big]=\frac{2\pi\hbar^2}{m}\frac{g^2}{2}\left\{-\frac{1}{2}+(kl)^2\,[5.402+3\ln(kl)]\right\}.$$

[1] K.-K. Ni, S. Ospelkaus, M. H. G. de Miranda, A. Pe’er, B. Neyenhuis, J. J. Zirbel, S. Kotochigova, P. S. Julienne, D. S. Jin, and J. Ye, Science **322**, 231 (2008).

[2] J. Deiglmayr, A. Grochola, M. Repp, K. Mörtlbauer, C. Glück, J. Lange, O. Dulieu, R. Wester, and M. Weidemüller, Phys. Rev. Lett. **101**, 133004 (2008).

[3] J. G. Danzl, M. J. Mark, E. Haller, M. Gustavsson, R. Hart, J. Aldegunde, J. M. Hutson, and H. C. Nägerl, Nature Phys. **6**, 265 (2010).

[4] K.-K. Ni, S. Ospelkaus, D. Wang, G. Quéméner, B. Neyenhuis, M. H. G. de Miranda, J. L. Bohn, J. Ye, and D. S. Jin, Nature (London) **464**, 1324 (2010).

[5] S. Ospelkaus, K.-K. Ni, D. Wang, M. H. G. de Miranda, B. Neyenhuis, G. Quéméner, P. S. Julienne, J. L. Bohn, D. S. Jin, and J. Ye, Science **327**, 853 (2010).

[6] M. H. G. de Miranda, A. Chotia, B. Neyenhuis, D. Wang, G. Quemener, S. Ospelkaus, J. L. Bohn, J. Ye, and D. S. Jin, e-print arXiv:1010.3731v1.

[7] R. Krems, B. Friedrich, and W. C. Stwalley (Eds.), *Cold Molecules: Theory, Experiment, Applications* (CRC Press, Boca Raton, FL, 2009).

[8] L. D. Carr, D. DeMille, R. V. Krems, and Jun Ye, New J. Phys. **11**, 055049 (2009); and papers in this special issue on polar molecules.

[9] M. A. Baranov, Phys. Rep. **464**, 71 (2008).

[10] T. Lahaye, C. Menotti, L. Santos, M. Lewenstein, and T. Pfau, Rep. Prog. Phys. **72**, 126401 (2009).

[11] A. Micheli, Z. Idziaszek, G. Pupillo, M. A. Baranov, P. Zoller, and P. S. Julienne, Phys. Rev. Lett. **105**, 073202 (2010).

[12] A. Pikovski, M. Klawunn, G. V. Shlyapnikov, and L. Santos, Phys. Rev. Lett. **105**, 215302 (2010).

[13] G. M. Bruun and E. Taylor, Phys. Rev. Lett. **101**, 245301 (2008).

[14] N. R. Cooper and G. V. Shlyapnikov, Phys. Rev. Lett. **103**, 155302 (2009).

[15] B. Simon, Ann. Phys. **97**, 279 (1976).

[16] S. M. Shih and D.-W. Wang, Phys. Rev. A **79**, 065603 (2009).

[17] J. R. Armstrong, N. T. Zinner, D. V. Fedorov, and A. S. Jensen, Europhys. Lett. **91**, 16001 (2010).

[18] M. Klawunn, A. Pikovski, and L. Santos, Phys. Rev. A **82**, 044701 (2010).

[19] N. T. Zinner, B. Wunsch, D. Pekker, and D.-W. Wang, e-print arXiv:1009.2030.

[20] H. P. Büchler, E. Demler, M. Lukin, A. Micheli, N. Prokof’ev, G. Pupillo, and P. Zoller, Phys. Rev. Lett. **98**, 060404 (2007).

[21] G. E. Astrakharchik, J. Boronat, I. L. Kurbakov, and Yu. E. Lozovik, Phys. Rev. Lett. **98**, 060405 (2007).

[22] L. D. Landau and E. M. Lifshitz, *Quantum Mechanics* (Butterworth-Heinemann, Oxford, 1999).

[23] D. S. Petrov and G. V. Shlyapnikov, Phys. Rev. A **64**, 012706 (2001).

[24] J. R. Taylor, *Scattering Theory* (John Wiley & Sons, New York, 1972).

[25] L. P. Gor’kov and T. K. Melik-Barkhudarov, Sov. Phys. JETP **13**, 1018 (1961).

[26] E. M. Lifshitz and L. P. Pitaevskii, *Statistical Physics* (Pergamon Press, Oxford, 1980), Part 2.

[27] J. P. Kestner and S. Das Sarma, Phys. Rev. A **82**, 033608 (2010).

[28] L. Sieberer and M. A. Baranov (in preparation).

[29] J. Levinsen, N. R. Cooper, and G. V. Shlyapnikov, e-print arXiv:1103.3859v1.

[30] D. S. Petrov, M. A. Baranov, and G. V. Shlyapnikov, Phys. Rev. A **67**, 031601R (2003).

[31] V. A. Khodel, V. V. Khodel, and J. W. Clark, Nucl. Phys. A **598**, 390 (1995).

[32] V. L. Berezinskii, Sov. Phys. JETP **34**, 610 (1972).

[33] J. M. Kosterlitz and D. J. Thouless, J. Phys. C **6**, 1181 (1973); J. M. Kosterlitz, *ibid.* **7**, 1046 (1974).

[34] K. Miyake, Prog. Theor. Phys. **69**, 1794 (1983).

[35] W. Ketterle and M. Zwierlein, in *Proceedings of the International School of Physics Enrico Fermi, Course CLXIV*, edited by M. Inguscio, W. Ketterle, and C. Salomon (IOS Press, Amsterdam, 2008), p. 95.